Received: 6 November 2024 | Revised: 13 December 2024 | Accepted: 4 January 2025

IET Renewable Power Generation

DOI: 10.1049/rpg2.13195

The Institution of Engineering and Technology WILEY

ORIGINAL RESEARCH

Integrating the strategic response of parking lots in active distribution networks: An equilibrium approach

Marcos Tostado-Véliz[1] | **Rohit Bhakar**[2] | **Mohammad Sadegh Javadi**[3] | **Ali Esmaeel Nezhad**[4] | **Francisco Jurado**[1]

[1]Department of Electrical Engineering, University of Jaén, Linares, Spain

[2]Department of Electrical Engineering, Malaviya National Institute of Technology, Jaipur, India

[3]Center for Power and Energy Systems, Institute for Systems and Computer Engineering, Technology and Science (INESC TEC), Porto, Portugal

[4]Department of Electrical Engineering, School of Energy Systems, LUT University, Lappeenranta, Finland

Correspondence
Francisco Jurado, Department of Electrical Engineering, University of Jaén, 23700 Linares, Spain.
Email: fjurado@ujaen.es

Funding information
Spanish Ministry of Science and Innovation, Grant/Award Number: PID2021-123633OB-C31; Institute for Systems and Computer Engineering, Technology and Science; INESC TEC

Abstract

The increasing penetration of electric vehicles will be accompanied for a wide deployment of charging infrastructures. Large charging demand brings formidable challenges to existing power networks, driving them near to their operational limits. In this regard, it becomes pivotal developing novel energy management strategies for active distribution networks that take into account the strategic behaviour of parking lots. This paper focuses on this issue, developing a novel energy management tool for distribution networks encompassing distributed generators and parking lots. The new proposal casts as a tri-level game equilibrium framework where the profit maximization of lots is implicitly considered, thus ensuring that network-level decisions do not detract the profit of parking owners. The original tri-level model is reduced into a tractable single-level mixed-integer-linear programming by combining equivalent primal-dual and first-order optimality conditions of the distribution network and parking operational models. This way, the model can be solved using off-the-shelf solvers, with superiority against other approaches like metaheuristics. The developed model is validated in well-known 33-, and 85-bus radial distribution systems. Results show that, even under unfavourable conditions with limited distributed generation, charging demand is maximized, thus preserving the interests of parking owners. Moreover, the model is further validated through a number of simulations, showing its effectiveness. Finally, it is demonstrated that the developed tool scales well with the size of the system, easing its implementation in real-life applications.

1 | INTRODUCTION

1.1 | Context and motivation

The European Commission targets carbon neutrality by 2050 [1]. To achieve such ambitious objective, different economy sectors need to be decarbonized rapidly. The mobility sector, which was responsible for 21% of total CO_2 emissions in Europe in 2021 [2], constitutes one of the most notorious examples. Decarbonizing the mobility sector requires replacing conventional combustion-based vehicles by electric alternatives, based on either batteries or fuel-cell storage technologies [3].

The massive integration of electric vehicles (EVs) must be accompanied by a proper charging infrastructure deployment, capable to supply an increasing number of EVs. Current charging technologies reach up to 250 kW of rating power, expecting to achieve up to 400 kW in a near future [4]. Integrating such demand into power networks supposes a challenge, driving existing infrastructures near to their operational limits [5].

Optimally planning and managing parking lots (PLs) may help to alleviate the negative impact of integrating charging infrastructures into existing networks. On the other hand, profitability of these installations needs to be maximized in order to encourage private investment in charging points, thus providing a proper infrastructure for a growing EV fleet [6]. This paper focuses on these issues.

1.2 | Literature review

Energy management and planning of PLs is not a new topic. A number of recent works have addressed this problem from different points of view such as uncertainty modelling [7], or market participation [8]. This paper, however, focuses on the integration of PLs in active distribution networks (ADNs). This topic is pivotal nowadays due to the challenges brought by PLs, as previously commented. In this regard, a number of works have recently focused on how to optimally design and manage PLs integrated in ADNs, proposing different approaches.

A number of references focus on optimal design of PLs integrated into ADNs. More specifically, the optimal sitting and sizing of PLs have been hot topics recently. Mirzaei et al. [9] develop a probabilistic approach for optimal sizing and sitting PLs in distribution networks. This approach employs the point-estimate-method to model uncertainties while reducing the computational burden caused by the number of scenarios considered. In particular, uncertain driving pattern is considered in order to properly size charging infrastructures. The authors in [10] propose an optimization model for sitting PLs in distribution networks, with focus on improving the economy of such infrastructures. The developed optimization model is solved using a genetic algorithm, showing that the optimal placement depends on different items such as number of EVs or electricity pricing. Likewise, Amini et al. [11] propose a two-stage methodology for simultaneous allocation of PLs and distributed generators (DGs) in ADNs, thus resulting in a collaborative approach. In particular, private investors propose possible allocations based on economic factors, while the distribution system operator (DSO) optimizes DGs at the second stage taking into account technical constraints of the network. Fathy and Abdelaziz [12] penned a comparison among different metaheuristics in optimal allocating and sizing PLs in ADNs. In particular, grey wolf, whale algorithm and water cycle optimizers are compared using a novel objective function encompassing reliability enhancement, power loss reduction and investment cost. A joint tool for optimal network expansion and PL placement is proposed in [13]. First, a probabilistic method is applied to determine EV driving and charging behaviour. This input serves to run a multi-objective optimization model, whose goal is determining expansion decisions and parking allocation considering economic and satisfaction factors. Yang et al. [14] employed a well-suited metaheuristic for optimal allocation and scheduling of wind turbines and PLs in distribution networks. The proposal casts as a many-objective optimization model, considering economy, degradation of batteries, energy purchased and power losses as objectives.

Integrating PLs with local generation resources such as photovoltaic (PV) panels can improve the economy and efficiency of the system. This issue was analysed in [15], where a methodology framework is proposed to assess the economic and technical viability of PLs in ADNs equipped with roof mounted PV arrays. Haghifam et al. [16] investigate a bi-level stochastic framework, for optimal day-ahead scheduling of ADNs in the presence of private microgrid and PL owners. The proposed model casts as a bi-level Stackelberg game framework in which the DSO plays as the leader and the other agents partake as followers. The same concept was applied in [17], where a bi-level strategy was proposed for distribution networks in the presence of PLs. In this case, the DSO aims at leveraging flexibility provided by EVs, for which tariff discounts can be offered in order to encourage users to partake actively in the operation of the system. Such initiatives can improve the peak-to-average ratio significantly. Haji-Aghajani et al. [18] employ a sorted genetic algorithm for optimal charging scheduling of PLs in distribution networks. The proposed model considers the point-estimate-method to model the probability of each vehicle entering in a particular lot, giving an uncertainty-aware feature to the results obtained. Nasiri et al. [19] develop a peer-to-peer transactive approach for distribution networks, involving networked microgrids and PLs. To this end, a local market mechanism is proposed, by which the different players exchange information with the market entity on the basis of local marginal prices. In order to preserve the privacy of users, the model is solved in a decentralized manner, using an alternating direction of multipliers algorithm.

The optimal charging management of EVs can improve the resilience of ADNs notably. This issue was investigated in [20], where a two-stage methodology for improving voltage imbalance in distribution systems was developed. This proposal includes the charging scheduling at first stage, considering users' satisfaction as well as the profit of charging points, whereas the second stage devoted on network operation. Results show that active participation of EVs may improve voltage imbalances by 30%. In [21], a novel energy management model was proposed focusing on determining optimal charging management and route profiles in order to improve the resiliency of networks under disturbances. Similarly, Khodadadi et al. [22] develop an optimization model to improve the resiliency of distribution networks hosting PLs. This model focuses on the impact of natural disasters, for which the authors developed an uncertainty-aware model which combines stochastic programming with Information Gap Decision Theory. Ref. [23] focuses on islanding formation with the objective of maximizing the level of load restoration in the presence of a grid disturbance. To this end, a bi-level model optimization model was proposed, by which PLs integrated in ADNs partake as active agents pursuing the resilient operation of the entire system. PLs may help in microgrid formation in order to enhance the reliability of distribution networks. This topic attracted attention in [24], where a two-stage stochastic optimization model was developed for enabling the participation of PLs in improving the reliability of grid infrastructures. To this end, earthquakes are modelled at first stage, using geographical data, whereas the second stage devotes on grid formation through a linear optimization model.

TABLE 1 A summary of the related literature.

Ref.	Model	Objective	DGs
[15]	Heuristic	Economic analysis	Yes (only PV)
[16, 17]	Stackelberg	Leader-followers economic optimization	Yes
[18]	Optimization	Drivers' willingness	Yes (only PV)
[19]	Distributed	Economic	Yes
Present	Equilibrium	Coordinated market	Yes

1.3 | Our point of view

References above present a variety of optimization-based methodologies devoted on either management or planning of PLs in distribution networks. Main differences among references lie in the specific focus of each work, including uncertainty modelling or resilience improving, as well as the solver employed, existing a number of different metaheuristics which have been tested under different scenarios.

It is worth mentioning the references [16, 17], which establish Stackelberg game approaches for the optimal coordination of PLs and the utility (the DSO, typically). Game-oriented approaches have some advantages, especially from an economic perspective, since allows incorporating the particular objectives of PLs into the operation of the grid. This ecosystem allows anticipating the response of private stakeholders who manage charging infrastructures, in order to look for equilibrium strategies among agents.

This paper moves forward this idea and conceptualize the distribution system as a local market, in which PLs play as strategic agents, thus forming a virtual oligopoly. Note that this idea has been already studied in conventional wholesale electricity markets [25], but its application to distribution systems hosting PLs results novel. In particular, we believe that considering this market arrangement features some important advantages compared to other approaches:

- Through this market mechanism, the DSO optimizes distributed resources anticipating the optimal response of PLs. This approach allows best scheduling distributed generators (DGs), improving the economy and efficiency of the system.
- It establishes an optimal ecosystem for encouraging private investment in charging infrastructures, considering the particular economy of PLs in the operation of the system and thus paving the way to increment the profit of stakeholders.
- It serves as a framework to further develop local market mechanisms. This way, the conceptual network model may help the DSO to take decisions regarding establishing local market rules, marginal prices or other different market alternatives.

For the sake of simplicity, Table 1 provides a brief comparison of the present paper with other literature related to energy management in ADNs with PLs. As seen, this paper contributes with an innovative distributed market based on equilibrium, by which the strategic response of PLs is concerned.

1.4 | Specific contributions and paper organization

The specific contributions of this paper are listed below:

- Developing optimization models for PLs and ADNs, focusing on improving the economy of the different agents. These models allow focusing on economy aspects, thus establishing valid optimization frameworks for a market perspective.
- Integrating the different agent models into a novel game-based tri-level game-oriented framework, in which PLs partake as strategic players reaching an equilibrium among them and the DSO. Note that this novel methodology differs notably of those in [16, 17], where PLs are considered as followers into conventional bi-level models.
- Reducing the developed game-based tri-level model into a tractable single-level one through an original combination of primal-dual formulations and first-order optimality conditions of the different agents.
- Validating the new proposal in well-known 33-, and 85-bus distribution systems, showing the impact of PLs in the operation of ADNs and concluding some important remarks regarding the benefits of applying the developed methodology for the DSO and PLs.

In the rest of this paper, Section 2 establishes the necessary background and states the proposed tri-level optimization framework. Section 3 presents the optimization models of the DSO and PLs. Section 4 describes the steps to reduce the original tri-level framework into a tractable single-level optimization model. Different cases studied with results are presented in Section 5. Finally, the paper is concluded with Section 6.

2 | BACKGROUND

2.1 | Basic notations

In the following, we use capital letters to denote sets, while small letters refer to the members within a set. Furthermore, cardinality of each set is expressed by means of its absolute value, i.e. $|\cdot|$.

We consider a radial distribution network formed by $|J|$ nodes, to which $|D|$ demands $|C|$ PLs are connected and supplied. Demands are assumed to be inflexible and PLs are private-owned and seek for optimizing their own profit by purchasing electricity from the network for charging EVs. On the other hand, DGs are directly connected to the network and can deliver power to satisfy local demand. Without loss of generality, DGs are divided into the sets G^{MT} and G^{RES}. The former encompasses microturbines (MTs), which are considered dispatchable and with an associated fuel cost, while the latter includes renewable generators encompassing PV arrays and wind farms, mainly. Finally, $|S|$ static var compensators (SVCs) are installed to provide reactive support.

In order to ease the notation, we consider the sets $\Omega_j^{D/G/C/S}$, which include the loads/generators/PLs/SVCs connected to

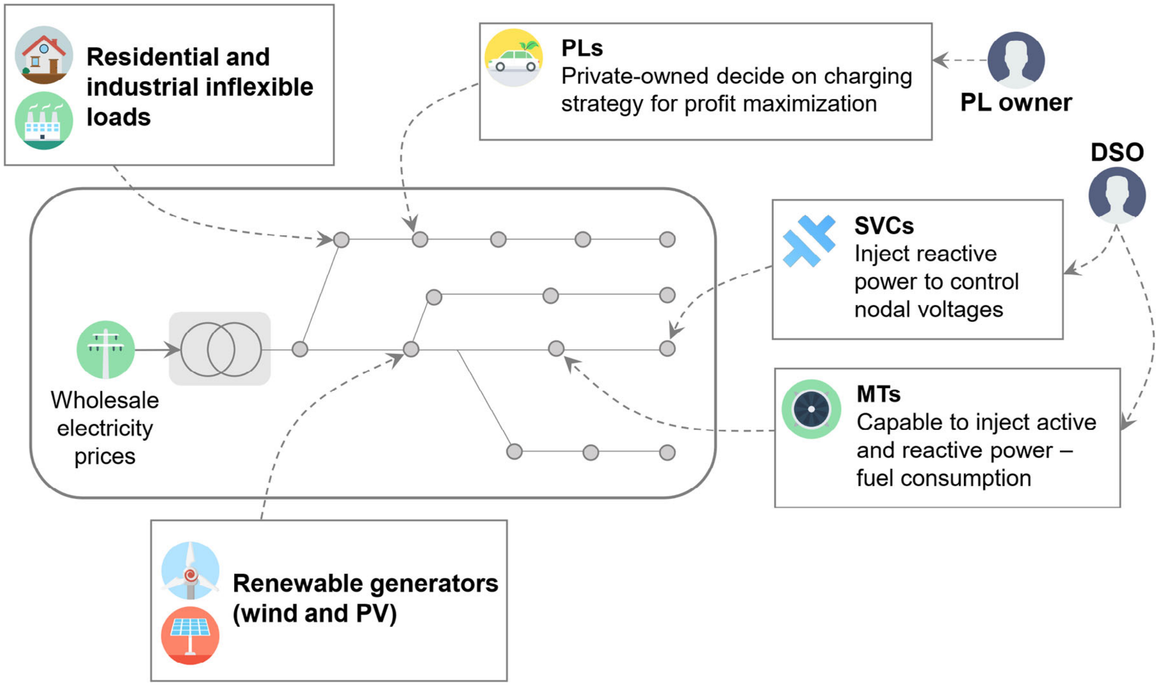

FIGURE 1 Sketch of the considered distribution network system.

the jth node in the network, respectively. Moreover, given the radiality of the network, the sets Ψ_j/Φ_j encompass the nodes downstream/upstream from the jth node in the network. Lastly, the notation J_ω indicates to which node the asset ω (i.e. demand, generators, PLs or SVCs) is connected.

2.2 | Network structure and operational fundamentals

The DSO is responsible of operating the network, ensuring that power flows and nodal voltages keep within secure limits. To this end, MTs and SVCs are directly operated by the DSO. On the other hand, PLs decide on their charging strategy in order to maximize their expected profit.

The ADN is connected to the transmission network at a root node, from which can exchange electricity at known wholesale electricity prices. Daily, PLs partake as strategic players, deciding their charging strategy on the basis of known electricity prices. In response to this strategy, the DSO decides on the scheduling plan for MTs and SVCs, forecasting inflexible demands with the objective of reducing the cost of operating the grid. Figure 1 sketches the considered ADN as well as the components and agents connected to.

2.3 | Problem statement

We consider an oligopoly local system in which PLs play as strategic firms. Similarly, such market arrangements have been studied in wholesale electricity markets, where large-scale generators are capable to exert market power by deciding on their offering strategy [26]. Mathematically, this problem casts as an equilibrium problem with equilibrium constraints (EPEC), as drawn in Figure 2. EPEC frameworks consider a number of strategic offer games, one for each strategy firm.

Individually, each strategic offering problem stands as a mathematical problem with equilibrium constraints (MPEC) [27]. MPECs are actually Stackelberg games where the strategic firm plays as the leader, while the network (or the market) plays as the follower. We translate this idea to the considered distribution system. In our particular case, PLs partake as strategic firms, while the network (in turn operated by the DSO) plays as the follower. Whilst, the considered mathematical framework constitutes a market arrangement suitable for maximizing the profit of PLs while seeking for reducing the cost of operating the network.

Furthermore, we pose a tri-level optimization model for the EPEC framework described above and sketched in Figure 2. At the low-level, the DSO aims at minimizing the operation cost while scheduling SVCs and MTs in order to operate the network in a safe manner. At the middle-level, each PL decides on charging strategy to maximize the expected profit, whereas ensuring a level of energy stored to satisfy the instantaneous charging demand. Each middle-low level is integrated constituting a MPEC, as detailed in Section 4. Finally, all the MPECs are jointly solved in an EPEC fashion, for which an auxiliary objective function is included (the network operating cost in this case).

The framework (1) writes in matrix form the market arrangement described above.

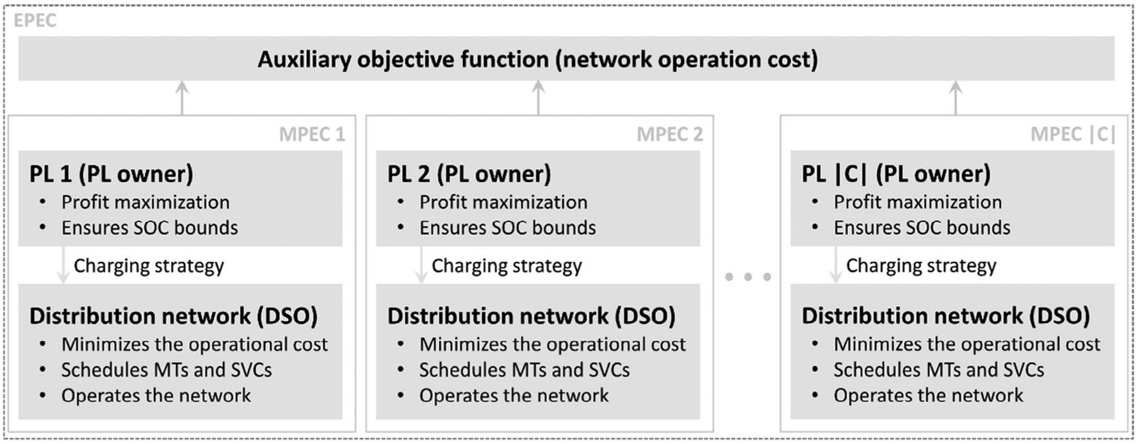

FIGURE 2 Conceptual scheme of the proposed EPEC framework.

$$\min_{\substack{\boldsymbol{x}^N,\boldsymbol{\lambda},\boldsymbol{\zeta},\boldsymbol{\psi},\\ \boldsymbol{x}_c,\boldsymbol{\phi}_c,\boldsymbol{\mu}_c;\forall c\in C}} NC \tag{1a}$$

$$\max_{\boldsymbol{x}^N,\boldsymbol{x}_c,\boldsymbol{\lambda},\boldsymbol{\zeta}} \text{Profit}_c; \forall c \in C \tag{1b}$$

Subject to:

$$\boldsymbol{h}_c\left(\boldsymbol{x}_c, \boldsymbol{x}^N, \boldsymbol{\lambda}, \boldsymbol{\zeta}\right) = 0 \ : \ \boldsymbol{\phi}_c; \forall c \in C \tag{1c}$$

$$\boldsymbol{g}_c\left(\boldsymbol{x}_c, \boldsymbol{x}^N, \boldsymbol{\lambda}, \boldsymbol{\zeta}\right) \leq 0 \ : \ \boldsymbol{\mu}_c; \forall c \in C \tag{1d}$$

$$\min_{\boldsymbol{x}^N} NC \tag{1e}$$

Subject to:

$$\boldsymbol{h}^N\left(\boldsymbol{x}^N\right) = 0 \ : \ \boldsymbol{\lambda} \tag{1f}$$

$$\boldsymbol{g}^N\left(\boldsymbol{x}^N\right) \leq 0 \ : \ \boldsymbol{\zeta} \tag{1g}$$

The high-level Equation (1a) is the EPEC model including the strategic action of all the agents in the distribution system. The EPEC problem includes the auxiliary objective function NC, which allows solving the model using conventional optimization techniques, as discussed later on. In this paper, we consider the operational cost of the network as coherent auxiliary function. The middle-level (1b)–(1d) corresponds to the PL-related problem, by which PLs seek to maximize their individual profit given in Profit_c. The middle-level incorporates typical operational constraints in Equations (1c) and (1d), concerning about physical limitations and power balances, mainly. Likewise, the low-level (1e)–(1g) minimizes the operational cost of the network under operational constraints. In Equation (1), dual-related variables are shown at the right-hand side of their corresponding equations. These variables allow replacing the middle and low-level problems by equivalent optimality conditions, as explained later on. Note that each problem decides on own variables $\boldsymbol{x}^N$ and $\boldsymbol{x}_c$, for the network and PLs, respectively. However, variables of lower levels are directly transferred to those at upper levels. This is a typical consequence of replacing lower-level problems by their optimality conditions, as explained in Section 4. Moreover, dual variables at lower levels are also transferred to upper levels.

3 | MATHEMATICAL MODELS

This section describes the mathematical modelling corresponding to PLs and the DSO. Both models cast as optimization problems focused on improving the economic of each stakeholder. As in Equation (1), dual variables are shown at the right-hand side of their corresponding constraints.

3.1 | The low-level

The low-level of the proposed tri-level framework (1) corresponds to the DSO, who schedules distributed assets (MTs and SVCs) in order to operate the network in a safe manner at minimum cost. The DSO is also responsible of trading energy with the transmission network under known wholesale electricity prices. The DSO model includes the network modelling. We assume a radial topology, as customary in distribution networks [28, 29], for which a linear power flow model can be adopted [30]. With such premises, the DSO model reads as:

$$\min_{\boldsymbol{x}^N} NC = \sum_{t\in T}\left\{ \mathrm{W}_t\left(p_t^{\text{im}} - a^{\text{ex}} p_t^{\text{ex}}\right) + \sum_{g\in G^{MT}} L_g p_{g,t} \right\} \tag{2a}$$

Subject to:

$$p_t^{\text{im}} - p_t^{\text{ex}} = f_{(j=0),t}^{P} : \lambda_t^{P,\text{sub}}; \forall t \in T \tag{2b}$$

$$q_t^{\text{im}} - q_t^{\text{ex}} = f_{(j=0),t}^{Q} : \lambda_t^{Q,\text{sub}}; \forall t \in T \tag{2c}$$

$$f_{j,t}^{P}=\sum_{d\in\Omega_j^D}p_{d,t}+\sum_{c\in\Omega_j^C}p_{c,t}-\sum_{g\in\Omega_j^G}p_{g,t}+\sum_{k\in\Psi_j}f_{k,t}^{P}\ :\ \lambda_{j,t}^{P};\forall j\in J\wedge t\in T \tag{2d}$$

$$f_{j,t}^{Q}=\sum_{d\in\Omega_j^D}q_{d,t}-\sum_{s\in\Omega_j^S}q_{s,t}-\sum_{g\in\Omega_j^G}q_{g,t}+\sum_{k\in\Psi_j}f_{k,t}^{Q}\ :\ \lambda_{j,t}^{Q};\forall j\in J\wedge t\in T \tag{2e}$$

$$V_{(j=0),t}=V^0:\lambda_{(j=0),t}^{V};\forall t\in T \tag{2f}$$

$$V_{j,t}=\sum_{k\in\Phi_j}V_{k,t}-\frac{R_jf_{j,t}^P+X_jf_{j,t}^Q}{V^0}\ :\ \lambda_{j,t}^{V};\forall j\in J\backslash\{0\}\wedge t\in T \tag{2g}$$

$$p_t^{\text{im}},p_t^{\text{ex}},q_t^{\text{im}},q_t^{\text{ex}}\geq 0\ :\ \underline{\zeta}_t^{P,\text{im}},\underline{\zeta}_t^{P,\text{ex}},\underline{\zeta}_t^{Q,\text{im}},\underline{\zeta}_t^{Q,\text{ex}};\forall t\in T \tag{2h}$$

$$\sqrt{\left(f_{j,t}^P\right)^2+\left(f_{j,t}^Q\right)^2}\leq\bar{f}_j;\forall j\in J\wedge t\in T \tag{2i}$$

$$0.95V^0\leq V_{j,y,s,t}\leq 1.05V^0:\ \underline{\zeta}_{j,t}^{V},\bar{\zeta}_{j,t}^{V};\forall j\in J\wedge t\in T \tag{2j}$$

$$\sqrt{\left(p_{g,t}\right)^2+\left(q_{g,t}\right)^2}\leq\bar{S}_g;\forall g\in G^{\text{MT}}\wedge t\in T \tag{2k}$$

$$p_{g,t}\leq\tilde{p}_{g,t}\ :\ \bar{\zeta}_{g,t};\forall g\in G^{\text{RES}}\wedge t\in T \tag{2l}$$

$$0\leq p_{g,t}\ :\ \underline{\zeta}_{g,t};\forall g\in G\wedge t\in T \tag{2m}$$

$$0\leq q_{s,t}\leq\bar{q}_s\ :\ \underline{\zeta}_{s,t},\bar{\zeta}_{s,t};\forall s\in S\wedge t\in T \tag{2n}$$

where $\boldsymbol{x}^N=\{p_t^{\text{im}},p_t^{\text{ex}},q_t^{\text{im}},q_t^{\text{ex}},f_{j,t}^P,f_{j,t}^Q,V_{j,t},p_{g,t},q_{g,t},q_{s,t}\}$.

The network operation cost (2a) is composed of two terms. Firstly, the cost of trading energy with the transmission networks under wholesale electricity prices W_t. The distribution system can leverage surplus generation and exporting it to the transmission network to obtain an income. In this work, we consider that selling prices are proportional to the purchasing ones [31], introducing a real constant $0<a^{\text{ex}}<1$. Secondly, the fuel cost of MTs is considered as a function of the total output of these generation units.

Active and reactive power balances at substation (root node) are given in Equations (2b) and (2c), respectively, while the nodal power balances are calculated in Equations (2d) and (2e) according to the linear power flow model adopted. Equation (2f) establishes the voltage at the root node, while Equation (2g) calculates the nodal voltages at the rest of nodes as a function of branch parameters and power flows across lines.

Inequality constraints comprise non-negativity of substation power flows in Equation (2h). Equation (2i) establishes thermal limits of branches, whereas Equation (2j) binds the nodal voltages to safe limits. Equation (2k) enforces power output of MTs to be below nominal power limit. The output of renewable generators is limited to forecasted potential in Equation (2l), while Equation (2m) imposes non-negativity in active power output of all the generators. Finally, Equation (2n) limits the reactive power injection of SVCs.

Model (2) is linear but Equations (2i) and (2k), which describe cone constraints. Although second order cone programming models can be solved straightforward using some advanced solvers like Gurobi [32], we propose here a simple linearization trick to enable solution of the proposed model easily by average solvers and machines. In this regard, we apply the inner-polygon approach, which has been successfully applied in other similar formulation [33, 34]. Thus, Equations (2i) and (2k) can be replaced by a set of $|N|$ linear equations of the form:

$$\gamma_n^Pf_{j,t}^P-\gamma_n^Qf_{j,t}^P-\gamma_n^f\bar{f}_j\leq 0\ :\ \bar{\xi}_{j,t,n}^{f};\forall j\in J\wedge t\in T\wedge n\in N \tag{2o}$$

$$\gamma_n^Pp_{g,t}-\gamma_n^Qq_{g,t}-\gamma_n^f\bar{S}_g\leq 0\ :\ \bar{\zeta}_{g,t,n};\forall g\in G^{\text{MT}}\wedge t\in T\wedge n\in N \tag{2p}$$

where the γ's are real parameters whose values can be calculated as detailed in [33]. Note that Equations (2o) and (2p) are not a relaxation, insofar that, enforcing the original set of constraints is equivalent to enforce Equations (2o) and (2p).

3.2 | The middle-level

As in [6], PLs are modelled as dynamic virtual battery systems following typical features of EVs. In this sense, PLs maximize their profit for charging while deciding on their charging strategy to keep the energy stored in the parking within limits, thus resulting in the following optimization model:

$$\max_{\boldsymbol{x}_c}\text{Profit}_c=\sum_{t\in T}F_cp_{c,t} \tag{3a}$$

Subject to:

$$\text{SOC}_{c,t}=\text{SOC}_{c,t-1}+C_{c,t}^0-\bar{C}_{c,t}^E+\eta p_{c,t}\ :\ \phi_{c,t}^{\text{SOC}};\forall t\in T\backslash\{1\} \tag{3b}$$

$$\text{SOC}_{c,(t=1)}=C_{c,(t=1)}^0:\phi_{c,(t=1)}^{\text{SOC}} \tag{3c}$$

$$\text{SOC}_{c,(t=|T|)}=\bar{C}_{c,|T|}^E:\phi_{c,|T|}^{\text{SOC}} \tag{3d}$$

$$\underline{\text{SOC}}_{c,t}\leq\text{SOC}_{c,t}\leq\overline{\text{SOC}}_{c,t}\ :\ \underline{\mu}_{c,t}^{\text{SOC}},\bar{\mu}_{c,t}^{\text{SOC}};\forall t\in T \tag{3e}$$

$$0\leq p_{c,t}\leq\bar{p}_{c,t}\ :\ \underline{\mu}_{c,t}^{p},\bar{\mu}_{c,t}^{p};\forall t\in T \tag{3f}$$

where $\boldsymbol{x}_c=\{\text{SOC}_{c,t},p_{c,t}\}$.

PLs aim at maximizing the charging power in Equation (3a) with charging price F_c. Equation (3b) expresses the energy

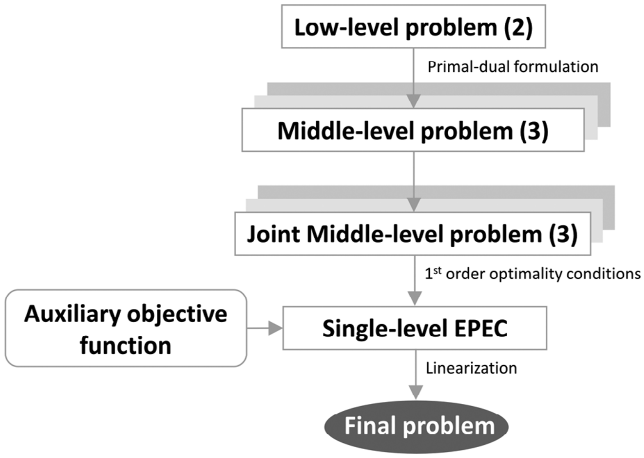

FIGURE 3 Steps for reducing the original tri-level problem (1) into a tractable single-level framework.

stored in the parking as a function of the energy stored at previous time step, the energy stored in vehicles arriving and leaving the parking and the total energy charged. Equation (3c) fixes the initial state-of-charge (SOC) as the energy stored in vehicles arriving at the beginning of the time horizon. Equation (3d) enforces that energy stored at the end of the time horizon must be sufficient to attend the demand of vehicles leaving the parking at the end of the day. Finally, Equations (3e) and (3f) enforce dynamic bounds in SOC and charging power, respectively. Note that limits in both Equations (3e) and (3f) depend on the vehicles plugged any time instant.

4 | REDUCTION TO A SINGLE-LEVEL PROBLEM

4.1 | Foundations

Solving multi-level optimization frameworks is a NP-hard problem [35]. Conventionally, this issue is circumvented by reducing the original multi-level structure into a tractable single-level one. To this end, lower-level problems are replaced by their first-order optimality conditions, encompassing stationary, feasibility and complementarity conditions (see [36]). While applying this approach in bi-level problems is straightforward, a different idea should be considered in tri-level frameworks as Equation (1). In this case, if the low-level is directly reduced to its first-order optimality conditions, the complementarity conditions would make the problem nonlinear and the joint middle-low-level could not be longer reduced, thus remaining as a hardy solvable bi-level problem.

To circumvent this issue, we apply the same idea as in [26]. Instead of replacing the low-level by its first-order optimality conditions, we consider an equivalent primal-dual formulation, which replaces complementarity conditions by the strong-duality equality, which can be easily linearized [37]. This way, the process of reducing Equation (1) to a single-level problem is sketched in Figure 3 and summarized in the following steps:

- Firstly, the low-level (2) is replaced by its equivalent primal-dual formulation and integrated into the middle-level, resulting in $|C|$ joint middle-low-level problems.
- Each joint middle-low-level is replaced by its equivalent first-order optimality conditions, resulting in an EPEC framework as depicted in Figure 2.
- An auxiliary objective function is included to convert the problem into a conventional optimization framework.
- Further nonlinearities are eliminated by applying different linearization tricks, as explained in Section 4.4.

4.2 | The joint middle-low-level problems

For each PL in the network there is an equivalent joint middle-low-level problem constituting its strategic participation. Each problem includes the original middle-level problem (3) along with the equivalent primal-dual formulation of the low-level problem (2), as follows:

$$\max_{\boldsymbol{x}^N,\boldsymbol{x}_c,\boldsymbol{\lambda},\boldsymbol{\zeta}} \ \text{Profit}_c = \sum_{t\in T} F_c p_{c,t} \tag{4a}$$

Subject to:

$$\text{Equations (3b)} - \text{(3f)} \tag{4b}$$

$$p_t^{\text{im}} - p_t^{\text{ex}} = f^P_{(j=0),t} : \phi_t^{P,\text{sub}}; \forall t \in T \tag{4c}$$

$$q_t^{\text{im}} - q_t^{\text{ex}} = f^Q_{(j=0),t} : \phi_t^{Q,\text{sub}}; \forall t \in T \tag{4d}$$

$$f^P_{j,t} = \sum_{d\in\Omega^D_j} p_{d,t} + \sum_{c\in\Omega^C_j} p_{c,t} - \sum_{g\in\Omega^G_j} p_{g,t} + \sum_{k\in\Psi_j} f^P_{k,t} \ : \ \phi^P_{j,t}; \forall j \in J \wedge t \in T \tag{4e}$$

$$f^Q_{j,t} = \sum_{d\in\Omega^D_j} q_{d,t} - \sum_{s\in\Omega^S_j} q_{s,t} - \sum_{g\in\Omega^G_j} q_{g,t} + \sum_{k\in\Psi_j} f^Q_{k,t} : \phi^Q_{j,t}; \forall j \in J \wedge t \in T \tag{4f}$$

$$V_{(j=0),t} = V^0 : \varphi^V_{(j=0),t}; \forall t \in T \tag{4g}$$

$$V_{j,t} = \sum_{k\in\Phi_j} V_{k,t} - \frac{R_j f^P_{j,t} + X_j f^Q_{j,t}}{V^0} \ : \ \varphi^V_{j,t}; \forall j \in J\setminus\{0\} \wedge t \in T \tag{4h}$$

$$\text{W}_t + \lambda_t^{P,\text{sub}} - \underline{\zeta}_t^{P,\text{im}} = 0 \ : \ \phi_t^{P,\text{im}}; \forall t \in T \tag{4i}$$

$$-a^{\text{ex}}\text{W}_t - \lambda_t^{P,\text{sub}} - \underline{\zeta}_t^{P,\text{ex}} = 0 \ : \ \phi_t^{P,\text{ex}}; \forall t \in T \tag{4j}$$

$$\lambda_t^{Q,\text{sub}} - \underline{\zeta}_t^{Q,\text{im}} = 0 \ : \ \phi_t^{Q,\text{im}}; \forall t \in T \tag{4k}$$

$$-\lambda_t^{Q,\text{sub}} - \underline{\zeta}_t^{Q,\text{ex}} = 0 : \phi_t^{Q,\text{ex}}; \forall t \in T \tag{4l}$$

$$-\lambda^P_{(j=0),t} - \lambda_t^{P,\text{sub}} + \sum_{n\in N} \gamma_n^P \bar{\zeta}^f_{(j=0),t,n} = 0 : \phi^{f^P}_{(j=0),t}; \forall t\in T \tag{4m}$$

$$-\lambda^P_{j,t} + \sum_{k\in\Phi_j}\lambda^P_{k,t} - \frac{\lambda^V_{j,t}R_j}{V^0} + \sum_{n\in N}\gamma_n^P\bar{\zeta}^f_{j,t,n} = 0 : \phi^{f^P}_{j,t}; \forall j\in J\backslash\{0\}\wedge t\in T \tag{4n}$$

$$-\lambda^Q_{(j=0),t} - \lambda_t^{Q,sub} - \sum_{n\in N}\gamma_n^Q\bar{\zeta}^f_{(j=0),t,n} = 0 : \phi^{f^Q}_{(j=0),t};\forall t\in T \tag{4o}$$

$$-\lambda^Q_{j,t} + \sum_{k\in\Phi_j}\lambda^Q_{k,t} - \frac{\lambda^V_{j,t}X_j}{V^0} - \sum_{n\in N}\gamma^Q_n\bar{\zeta}^f_{j,t,n} = 0 : \phi^{f^Q}_{j,t}; \forall j\in J\backslash\{0\}\wedge t\in T \tag{4p}$$

$$-V^0\lambda^V_{(j=0),t} + \sum_{k\in\Psi_{(j=0)}}\lambda^V_{k,t} - \underline{\zeta}^V_{(j=0),t} + \bar{\zeta}^V_{(j=0),t} = 0 : \phi^V_{(j=0),t};\forall t\in T \tag{4q}$$

$$-\lambda^V_{j,t} + \sum_{k\in\Psi_j}\lambda^V_{k,t} - \underline{\zeta}^V_{j,t} + \bar{\zeta}^V_{j,t} = 0 : \phi^V_{j,t};\forall j\in J\backslash\{0\}\wedge t\in T \tag{4r}$$

$$L_g - \lambda^P_{(j=J_g),t} + \sum_{n\in N}\gamma_n^P\bar{\zeta}_{g,t,n} - \underline{\zeta}_{g,t} = 0 : \phi^P_{g,t};\forall g\in G^{MT}\wedge t\in T \tag{4s}$$

$$-\lambda^P_{(j=J_g),t} - \underline{\zeta}_{g,t} + \bar{\zeta}_{g,t} = 0 : \phi^P_{g,t}; \forall g\in G^{RES}\wedge t\in T \tag{4t}$$

$$-\lambda^Q_{(j=J_g),t} - \sum_{n\in N}\gamma^Q_n\bar{\zeta}_{g,t,n} = 0 : \phi^Q_{g,t};\forall g\in G^{MT}\wedge t\in T \tag{4u}$$

$$-\lambda^Q_{(j=J_s),t} - \underline{\zeta}_{s,t} + \bar{\zeta}_{s,t} = 0 : \phi^Q_{s,t};\forall s\in S\wedge t\in T \tag{4v}$$

$$\begin{aligned} NC = \sum_{t\in T}\Bigg\{ & \sum_{j\in J}\Bigg\{\lambda^P_{j,t}\Bigg(\sum_{d\in\Omega^D_j} p_{d,t} + \sum_{c\in\Omega^C_j} p_{c,t}\Bigg) + \lambda^Q_{j,t}\sum_{d\in\Omega^D_j} q_{d,t} \\ & - \sum_{n\in N}\gamma_n^f \bar{f}_j \bar{\zeta}^f_{j,t,n} + 0.95V^0\underline{\zeta}^V_{j,t} - 1.05V^0\bar{\zeta}^V_{j,t}\Bigg\} \\ & - \sum_{g\in G^{MT}}\sum_{n\in N}\gamma_n^f \bar{S}_g\bar{\zeta}_{g,t,n} - \sum_{g\in G^{RES}}\tilde{p}_{g,t}\bar{\zeta}_{g,t} \\ & - \sum_{s\in S}\bar{q}_s\bar{\zeta}_{s,t} - V^0\lambda^V_{(j=0),t}\Bigg\} : \phi^{SD} \end{aligned} \tag{4w}$$

$$\begin{aligned} & \underline{\zeta}_t^{P,\text{im}}, \underline{\zeta}_t^{P,\text{ex}}, \underline{\zeta}_t^{Q,\text{im}}, \underline{\zeta}_t^{Q,\text{ex}}, \bar{\zeta}^f_{j,t,n}, \underline{\zeta}^V_{j,t}, \bar{\zeta}^V_{j,t}, \underline{\zeta}_{g,t}, \bar{\zeta}_{g,t}, \bar{\zeta}_{g,t,n}, \underline{\zeta}_{s,t}, \bar{\zeta}_{s,t} \\ & \geq 0 : \underline{\mu}_t^{P,\text{im}}, \underline{\mu}_t^{P,\text{ex}}, \underline{\mu}_t^{Q,\text{im}}, \underline{\mu}_t^{Q,\text{ex}}, \bar{\mu}^f_{j,t,n}, \underline{\mu}^V_{j,t}, \bar{\mu}^V_{j,t}, \underline{\mu}_{g,t}, \bar{\mu}_{g,t}, \\ & \bar{\mu}_{g,t,n}, \underline{\mu}_{s,t}, \bar{\mu}_{s,t}; \forall j\in J\wedge g\in G\wedge s\in S\wedge t\in T\wedge n\in N \end{aligned} \tag{4x}$$

$$\boldsymbol{\lambda} : \text{free} \tag{4y}$$

where $\boldsymbol{\lambda} = \{\lambda_t^{P,\text{sub}}, \lambda_t^{Q,\text{sub}}, \lambda^P_{j,t}, \lambda^Q_{j,t}, \lambda^V_{j,t}\}$ and $\boldsymbol{\zeta} = \{\underline{\zeta}_t^{P,\text{im}}, \underline{\zeta}_t^{P,\text{ex}}, \underline{\zeta}_t^{Q,\text{im}}, \underline{\zeta}_t^{Q,\text{ex}}, \bar{\zeta}^f_{j,t,n}, \underline{\zeta}^V_{j,t}, \bar{\zeta}^V_{j,t}, \underline{\zeta}_{g,t}, \bar{\zeta}_{g,t}, \bar{\zeta}_{g,t,n}, \underline{\zeta}_{s,t}, \bar{\zeta}_{s,t}\}$.

As seen, Equations (4) and (3) share the same objective function (i.e. profit maximization of the parking), but Equation (4) expands the decision variable-space to include the dual variables of the low-level. The joint middle-low-level includes the original constraints of the middle-level problem in Equation (4b) and the equivalent primal-dual formulation of the low-level one, formed by its feasibility constraints (4b)-(4h), its stationary conditions (4i)-(4v), the strong-duality equality (4w) and its dual feasibility constraints (4x) and (4y).

It is worth noting that Equation (4) does not include complementarity conditions and thus the joint middle-low-level problems are linear but the strong-duality equality, which can be easily linearized as explained in Section 4.4.

4.3 | The single-level EPEC problem

To solve all the joint middle-low-level problems in an EPEC fashion, each framework (4) is replaced by its equivalent first-order optimality conditions, given below:

$$\phi_t^{P,\text{sub}} + \mathrm{W}_t\,\phi^{\text{SD}} = 0; \forall t\in T \tag{5a}$$

$$-\phi_t^{P,\text{sub}} - a^{\text{ex}}\mathrm{W}_t\,\phi^{\text{SD}} = 0; \forall t\in T \tag{5b}$$

$$\phi_t^{Q,\text{sub}} = 0; \forall t\in T \tag{5c}$$

$$-\phi_t^{Q,\text{sub}} = 0; \forall t\in T \tag{5d}$$

$$-\phi^P_{(j=0),t} - \phi_t^{P,\text{sub}} = 0; \forall t\in T \tag{5e}$$

$$-\phi^P_{j,t} + \sum_{k\in\Phi_j}\phi^P_{k,t} - \frac{\varphi^V_{j,t}R_j}{V^0} = 0; \forall j\in J\backslash\{0\}\wedge t\in T \tag{5f}$$

$$-\phi^Q_{(j=0),t} - \phi_t^{Q,\text{sub}} = 0; \forall t\in T \tag{5g}$$

$$-\phi^Q_{j,t} + \sum_{k\in\Phi_j}\phi^Q_{k,t} - \frac{\varphi^V_{j,t}X_j}{V^0} = 0; \forall j\in J\backslash\{0\}\wedge t\in T \tag{5h}$$

$$-V^0\varphi^V_{(j=0),t} + \sum_{k\in\Psi_{(j=0)}}\varphi^V_{k,t} = 0; \forall j\in J\wedge t\in T \tag{5i}$$

$$-\varphi_{j,t}^{V}+\sum_{k\in\Psi_j}\varphi_{k,t}^{V}=0;\forall j\in J\wedge t\in T \tag{5j}$$

$$-\phi_{(j=J_g),t}^{P}+L_g\phi^{\mathrm{SD}}=0;\forall g\in G^{\mathrm{MT}}\wedge t\in T \tag{5k}$$

$$-\phi_{(j=J_g),t}^{P}=0;\forall g\in G^{\mathrm{RES}}\wedge t\in T \tag{5l}$$

$$-\phi_{(j=J_g),t}^{Q}=0;\forall g\in G^{\mathrm{MT}}\wedge t\in T \tag{5m}$$

$$-\phi_{(j=J_s),t}^{Q}=0;\forall s\in S\wedge t\in T \tag{5n}$$

$$-F_c-\eta\phi_{c,t}^{\mathrm{SOC}}+\phi_{(j=\Theta_c),t}^{f^P}-\lambda_{(j=J_c),t}^{P}\phi^{\mathrm{SD}}-\underline{\mu}_{c,t}^{p}+\bar{\mu}_{c,t}^{p}=0;\forall t\in T \tag{5o}$$

$$\phi_{c,t}^{\mathrm{SOC}}-\phi_{c,t+1}^{\mathrm{SOC}}-\underline{\mu}_{c,t}^{\mathrm{SOC}}+\bar{\mu}_{c,t}^{\mathrm{SOC}}=0;\forall t\in T\setminus\{|T|\} \tag{5p}$$

$$\phi_{c,(t=|T|)}^{\mathrm{SOC}}+\phi_{c,|T|}^{\mathrm{SOC}}-\underline{\mu}_{c,(t=|T|)}^{\mathrm{SOC}}+\bar{\mu}_{c,(t=|T|)}^{\mathrm{SOC}}=0 \tag{5q}$$

$$\phi_t^{P,\mathrm{im}}-\phi_t^{P,\mathrm{ex}}-\phi_{(j=0),t}^{f^P}=0;\forall t\in T \tag{5r}$$

$$\phi_t^{Q,\mathrm{im}}-\phi_t^{Q,\mathrm{ex}}-\phi_{(j=0),t}^{f^Q}=0;\forall t\in T \tag{5s}$$

$$-\phi_{j,t}^{f^P}+\sum_{k\in\Psi_j}\phi_{k,t}^{f^P}-\sum_{g\in\Omega_j^G}\phi_{g,t}^{P}-\phi^{\mathrm{SD}}\left(\sum_{d\in\Omega_j^D}p_{d,t}+\sum_{c\in\Omega_j^C}p_{c,t}\right)=0;\forall j\in J\wedge t\in T \tag{5t}$$

$$-\phi_{j,t}^{f^Q}+\sum_{k\in\Psi_j}\phi_{k,t}^{f^Q}-\sum_{g\in\Omega_j^G}\phi_{g,t}^{Q}-\phi^{\mathrm{SD}}\sum_{d\in\Omega_j^D}q_{d,t}=0;\forall j\in J\wedge t\in T \tag{5u}$$

$$-V^0\phi_{(j=0),t}^{V}+V^0\phi^{\mathrm{SD}}=0;\forall t\in T \tag{5v}$$

$$-\phi_{j,t}^{V}-\frac{\phi_{j,t}^{f^P}R_j}{V^0}-\frac{\phi_{j,t}^{f^Q}X_j}{V^0}+\sum_{k\in\Phi_j}\phi_{k,t}^{V}=0;\forall j\in J\setminus\{0\}\wedge t\in T \tag{5w}$$

$$-\phi_t^{P,\mathrm{im}}-\underline{\mu}_t^{P,\mathrm{im}}=0;\forall t\in T \tag{5x}$$

$$-\phi_t^{P,\mathrm{ex}}-\underline{\mu}_t^{P,\mathrm{ex}}=0;\forall t\in T \tag{5y}$$

$$-\phi_t^{Q,\mathrm{im}}-\underline{\mu}_t^{Q,\mathrm{im}}=0;\forall t\in T \tag{5z}$$

$$-\phi_t^{Q,\mathrm{ex}}-\underline{\mu}_t^{Q,\mathrm{ex}}=0;\forall t\in T \tag{5aa}$$

$$\gamma_n^P\phi_{j,t}^{f^P}-\gamma_n^Q\phi_{j,t}^{f^Q}+\gamma_n^f\bar{f}_g\phi^{\mathrm{SD}}-\bar{\mu}_{j,t,n}^{f}=0;\forall j\in J\wedge t\in T\wedge n\in N \tag{5ab}$$

$$-\phi_{j,t}^{V}-0.95V^0\phi^{\mathrm{SD}}-\underline{\mu}_{j,t}^{V}=0;\forall j\in J\wedge t\in T \tag{5ac}$$

$$-\phi_{j,t}^{V}+1.05V^0\phi^{\mathrm{SD}}-\bar{\mu}_{j,t}^{V}=0;\forall j\in J\wedge t\in T \tag{5ad}$$

$$-\phi_{g,t}^{P}-\underline{\mu}_{g,t}=0;\forall g\in G\wedge t\in T \tag{5ae}$$

$$\gamma_n^P\phi_{j,t}^{P}-\gamma_n^Q\phi_{j,t}^{Q}+\gamma_n^f\bar{S}_g\phi^{SD}-\bar{\mu}_{g,t,n}=0;\forall g\in G^{MT}\wedge t\in T\wedge n\in N \tag{5af}$$

$$\phi_{g,t}^{P}+\tilde{p}_{g,t}\phi^{\mathrm{SD}}-\bar{\mu}_{g,t}=0;\forall g\in G^{\mathrm{RES}}\wedge t\in T \tag{5ag}$$

$$-\phi_{s,t}^{Q}-\underline{\mu}_{s,t}=0;\forall s\in S\wedge t\in T \tag{5ah}$$

$$\phi_{s,t}^{Q}+\bar{q}_s\phi^{\mathrm{SD}}-\bar{\mu}_{s,t}=0;\forall s\in S\wedge t\in T \tag{5ai}$$

$$0\le \mathrm{SOC}_{c,t}-\underline{\mathrm{SOC}}_{c,t}\perp\underline{\mu}_{c,t}^{\mathrm{SOC}}\ge 0;\forall t\in T \tag{5aj}$$

$$0\le \overline{\mathrm{SOC}}_{c,t}-\mathrm{SOC}_{c,t}\perp\bar{\mu}_{c,t}^{\mathrm{SOC}}\ge 0;\forall t\in T \tag{5ak}$$

$$0\le p_{c,t}\perp\underline{\mu}_{c,t}^{p}\ge 0;\forall t\in T \tag{5al}$$

$$0\le \bar{p}_{c,t}-p_{c,t}\perp\bar{\mu}_{c,t}^{p}\ge 0;\forall t\in T \tag{5am}$$

$$0\le \underline{\zeta}_t^{P,\mathrm{im}}\perp\underline{\mu}_t^{P,\mathrm{im}}\ge 0;\forall t\in T \tag{5an}$$

$$0\le \underline{\zeta}_t^{P,\mathrm{ex}}\perp\underline{\mu}_t^{P,\mathrm{ex}}\ge 0;\forall t\in T \tag{5ao}$$

$$0\le \underline{\zeta}_t^{Q,\mathrm{im}}\perp\underline{\mu}_t^{Q,\mathrm{im}}\ge 0;\forall t\in T \tag{5ap}$$

$$0\le \underline{\zeta}_t^{Q,\mathrm{ex}}\perp\underline{\mu}_t^{Q,\mathrm{ex}}\ge 0;\forall t\in T \tag{5aq}$$

$$0\le \bar{\zeta}_{j,t,n}^{f}\perp\bar{\mu}_{j,t,n}^{f}\ge 0;\forall j\in J\wedge t\in T\wedge n\in N \tag{5ar}$$

$$0\le \underline{\zeta}_{j,t}^{V}\perp\underline{\mu}_{j,t}^{V}\ge 0;\forall j\in J\wedge t\in T \tag{5as}$$

$$0\le \bar{\zeta}_{j,t}^{V}\perp\bar{\mu}_{j,t}^{V}\ge 0;\forall j\in J\wedge t\in T \tag{5at}$$

$$0\le \underline{\zeta}_{g,t}\perp\underline{\mu}_{g,t}\ge 0;\forall g\in G\wedge t\in T \tag{5au}$$

$$0\le \bar{\zeta}_{g,t,n}\perp\bar{\mu}_{g,t,n}\ge 0;\forall g\in G^{\mathrm{MT}}\wedge t\in T \tag{5av}$$

$$0\le \bar{\zeta}_{g,t}\perp\bar{\mu}_{g,t}\ge 0;\forall g\in G^{\mathrm{RES}}\wedge t\in T \tag{5aw}$$

$$0\le \underline{\zeta}_{s,t}\perp\underline{\mu}_{s,t}\ge 0;\forall s\in S\wedge t\in T \tag{5ax}$$

$$0\le \bar{\zeta}_{s,t}\perp\bar{\mu}_{s,t}\ge 0;\forall s\in S\wedge t\in T \tag{5ay}$$

$$\boldsymbol{\lambda}, \boldsymbol{\phi}_c : \text{free} \tag{5az}$$

$$\boldsymbol{\mu}_c \geq 0 \tag{5ba}$$

where $\boldsymbol{\phi}_c = \{\phi^{\text{SD}}, \phi^{\text{SOC}}_{c,t}, \phi^{P,\text{sub}}_t, \phi^{Q,\text{sub}}_t, \phi^{P}_{j,t}, \phi^{Q}_{j,t}, \varphi^{V}_{j,t}, \phi^{P,\text{im}}_t, \phi^{P,\text{ex}}_t, \phi^{Q,\text{im}}_t, \phi^{Q,\text{ex}}_t, \phi^{f^P}_{j,t}, \phi^{f^Q}_{j,t}, \phi^{V}_{j,t}, \phi^{P}_{g,t}, \phi^{Q}_{g,t}, \phi^{Q}_{s,t}\}$ and $\boldsymbol{\mu}_c = \{\underline{\mu}^{P,\text{im}}_t, \underline{\mu}^{P,\text{ex}}_t, \underline{\mu}^{Q,\text{im}}_t, \underline{\mu}^{Q,\text{ex}}_t, \bar{\mu}^{f}_{j,t,n}, \underline{\mu}^{V}_{j,t}, \bar{\mu}^{V}_{j,t}, \underline{\mu}_{g,t}, \bar{\mu}_{g,t}, \bar{\mu}_{g,t,n}, \underline{\mu}_{s,t}, \bar{\mu}_{s,t}, \underline{\mu}^{\text{SOC}}_{c,t}, \bar{\mu}^{\text{SOC}}_{c,t}, \underline{\mu}^{p}_{c,t}, \bar{\mu}^{p}_{c,t}\}$.

The formulation above includes the stationary (5a)–(5ai), complementarity (5aj)–(5ay) and dual feasibility (5az), (5ba) conditions, of the cth PL in the network. Thus, the resulting EPEC is formed by $|C|$ problems of the form of Equation (5) which can be solved using an auxiliary objective function and including the equality constraints arisen in Equations (2)–(4) [38]. However, such formulation results nonlinear due to the strong-duality equality (4w), the complementarity conditions (5aj)–(5ay) and the bilinear terms in Equations (5o) and (5t) due to the presence of ϕ^{SD}. In the following subsection, we detail different linearization tricks to eliminate such nonlinearities, thus resulting in a tractable single-level mixed integer linear programming (MILP).

4.4 | Linearization

To linearize the complementarity conditions (5aj)–(5ay), the big-M approach can be applied [39], by which such conditions can be replaced by the following set of mixed-integer-linear constraints:

$$0 \leq b_1 \perp b_2 \geq 0 \rightarrow \begin{cases} b_1 \leq \psi M \\ b_2 \leq (1-\psi)\, M \\ \psi \in \{0,1\} \end{cases} \tag{6}$$

where $b_1, b_1 \in \mathfrak{R}_+$. The equivalence (6) is exact if the big-M's are tuned properly. Frequently, tuning these constants is challenging and case-dependent [40]. However, as our problem does not include economic variables, these constants can be chosen arbitrarily high (e.g. 10^6).

The strong-duality equality (4w) can be replaced by its equivalent complementarity conditions given below:

$$0 \leq p^{\text{im}}_t \perp \underline{\zeta}^{P,\text{im}}_t \geq 0; \forall t \in T \tag{7a}$$

$$0 \leq p^{\text{ex}}_t \perp \underline{\zeta}^{P,\text{ex}}_t \geq 0; \forall t \in T \tag{7b}$$

$$0 \leq q^{\text{im}}_t \perp \underline{\zeta}^{Q,\text{im}}_t \geq 0; \forall t \in T \tag{7c}$$

$$0 \leq q^{\text{ex}}_t \perp \underline{\zeta}^{Q,\text{ex}}_t \geq 0; \forall t \in T \tag{7d}$$

$$0 \leq \gamma^Q_n f^Q_{j,t} + \gamma^f_n \bar{f}_j - \gamma^P_n f^P_{j,t} \perp \bar{\zeta}^f_{j,t,n} \geq 0; \forall j \in J \wedge t \in T \wedge n \in N \tag{7e}$$

$$0 \leq V_{j,t} - 0.95V^0 \perp \underline{\zeta}^V_{j,t} \geq 0; \forall j \in J \wedge t \in T \tag{7f}$$

$$0 \leq 1.05V^0 - V_{j,t} \perp \underline{\zeta}^V_{j,t} \geq 0; \forall j \in J \wedge t \in T \tag{7g}$$

$$0 \leq p_{g,t} \perp \underline{\zeta}_{g,t} \geq 0; \forall g \in G \wedge t \in T \tag{7h}$$

$$0 \leq \tilde{p}_{g,t} - p_{g,t} \perp \bar{\zeta}_{g,t} \geq 0; \forall g \in G^{\text{RES}} \wedge t \in T \tag{7i}$$

$$0 \leq \gamma^Q_n q_{g,t} + \gamma^f_n \bar{S}_g - \gamma^P_n p_{g,t} \perp \bar{\zeta}_{g,t} \geq 0; \forall g \in G^{\text{MT}} \wedge t \in T \wedge n \in N \tag{7j}$$

$$0 \leq q_{s,t} \perp \underline{\zeta}_{s,t} \geq 0; \forall s \in S \wedge t \in T \tag{7k}$$

$$0 \leq \bar{q}_{s,t} - q_{s,t} \perp \bar{\zeta}_{s,t} \geq 0; \forall s \in S \wedge t \in T \tag{7l}$$

Note that Equation (7) can be linearized using Equation (6). Finally, bilinear terms in Equations (5o) and (5t) are omitted by parametrizing ϕ^{SD}. In our particular case, we found that setting $\phi^{\text{SD}} = 0$ usually gives valid results.

4.5 | Final MILP

After applying the linearization tricks in Section 4.4, the resulting single level MILP reads as:

$$\min_{\substack{\boldsymbol{x}^N, \boldsymbol{\lambda}, \boldsymbol{\zeta}, \boldsymbol{\psi}, \\ \boldsymbol{x}_c, \boldsymbol{\phi}_c, \boldsymbol{\mu}_c; \forall c \in C}} \quad NC \tag{8a}$$

Subject to:

$$\text{Equations (2b)} - \text{(2g)} \tag{8b}$$

$$\text{Equations (3b)} - \text{(3d)}\ ; \forall c \in C \tag{8c}$$

$$\text{Equations (4i)} - \text{(4v)} \tag{8d}$$

$$\text{Equations (5a)} - \text{(5ai)}\ ; \forall c \in C \tag{8e}$$

$$\text{(5az)}, \text{(5ba)} \tag{8g}$$

$$\boldsymbol{\Gamma}\left(\boldsymbol{x}^N, \boldsymbol{x}_c, \boldsymbol{\zeta}, \boldsymbol{\mu}_c\right) \leq \boldsymbol{\psi} M \tag{8h}$$

where $\boldsymbol{\psi}$ includes all the binary variables in Equation (6).

The problem (8) includes the equality constraints of the low and middle-level problems in Equations (8b) and (8c), respectively. Equation (8d) are the equality constraints of the primal-dual equivalent formulation of the low-level problem. Equations (8e) and (8g) include the stationary and dual feasibility conditions of each joint middle-low-level problem, respectively; whereas Equation (8h) encompasses the linearized complementarity conditions Equations (5aj)–(5ay) and (7) following the equivalent linear formulation (6).

It is worth noting that Equation (8) includes an auxiliary objective function (8a). In our case, the minimization of the network operation cost has been chosen, assuming that the objective of PLs is implicitly included in their first-order optimality conditions. This way, both objectives are actually considered on a whole. Moreover, we have observed that choosing a dummy objective function as in [38] gives rise similar results, thus validating our adoption.

4.6 | Limitations

The final model (8) constitutes a tractable optimization model, which could be solved efficiently using off-the-shelf solvers (see computational analysis in Section 5.5), Thereby, we consider that our proposal could be implemented in industrial tools easily. Nevertheless, we call the reader attention on two limitations that will be addressed in future works:

- Solving the model (8) requires sharing information between PLs and the network, by including primal constraints. As such, the application of the developed model may entail privacy issues. This issue could be circumvented by studying data-markets by which individuals could obtain a benefit by sharing data (see [41]).
- The power-flow model is linear and only applicable to radial distribution networks, which limits its applicability in meshed grids. Nevertheless, it is important to note that the new proposal is devoted on distribution networks, which are radial typically. Thus, future works will study alternative models to be applied in a variety of systems.

5 | NUMERICAL RESULTS

This section presents different cases studied with results, taking a 24-h time window with 1-h time resolution. The developed MILP (8) has been coded under Matlab R2021b and solved using Gurobi [32].

5.1 | Cases studied

In order to validate the developed method and taking the network described in Section 2.1 as benchmark, we evaluate and compare the results obtained under the different cases studied:

- Case 1: it is considered the base case in which MTs and renewable distributed generators are active and can contribute to minimizing the total network cost.
- Case 2: MTs are disabled so that local generation is only enabled through renewable generators.
- Case 3: renewable generators are disabled so that local generation is only enabled through MTs.

The developed methodology is thus validated in two ADN models with 33 and 85 nodes. We validate the integrated model proposed by observing some key results related to power trading and cost analysis, while the network modelling is validated analysing the voltage profile across the network. In addition, we provide a sensitivity analysis regarding the level of demand and renewable penetration. The developed computational tool is validated for industry tools by analysis its performance as well as comparing it with other optimization approaches like metaheuristics.

TABLE 2 ECs peal powers in the 33-bus case.

Node	Peak power (kW)	Node	Peak power (kW)
@1	150	@18	400
@2	200	@20	550
@3	250	@22	450
@6	150	@25	275
@8	200	@27	190
@9	200	@29	250
@12	150	@30	200
@14	150	@32	250
@16	100		

TABLE 3 Renewable generators nominal power in the 33-bus case.

Node	Nominal power (kW)
@5	300
@11	400
@24	300
@28	450

5.2 | The 33-bus case

We firstly consider the modified 12.66 kV radial 33-bus distribution network as depicted in Figure 4, with branch data extracted from [42]. We consider both residential and industrial loads, whose base profiles are given in Figure 5 and based on those considered in [43]. As seen, residential load profile follows typical demand curves in residential areas, with peak demand at morning and evening. In contrast, industrial demand achieves its maximum at midday, following working routines, while the demand for the rest of the day is very low. Profiles in Figure 5 are given in per-unit, to obtain the demand in kW, they have to be multiplied by the peak powers reported in Table 2. Reactive power consumption of each load is a fixed 10% and 30% of the active load for residential and industrial consumers, respectively, which is coherent with typical devices in such installations.

Renewable PV and wind generators are installed at nodes 5, 11, 24, and 28, with nominal power given in Table 3 and whose per-unit potential detailed in Figure 5, which are extracted from real data in [44]. The wholesale electricity price is plotted in Figure 5 responding to the real-time prices for the PJM in [31],

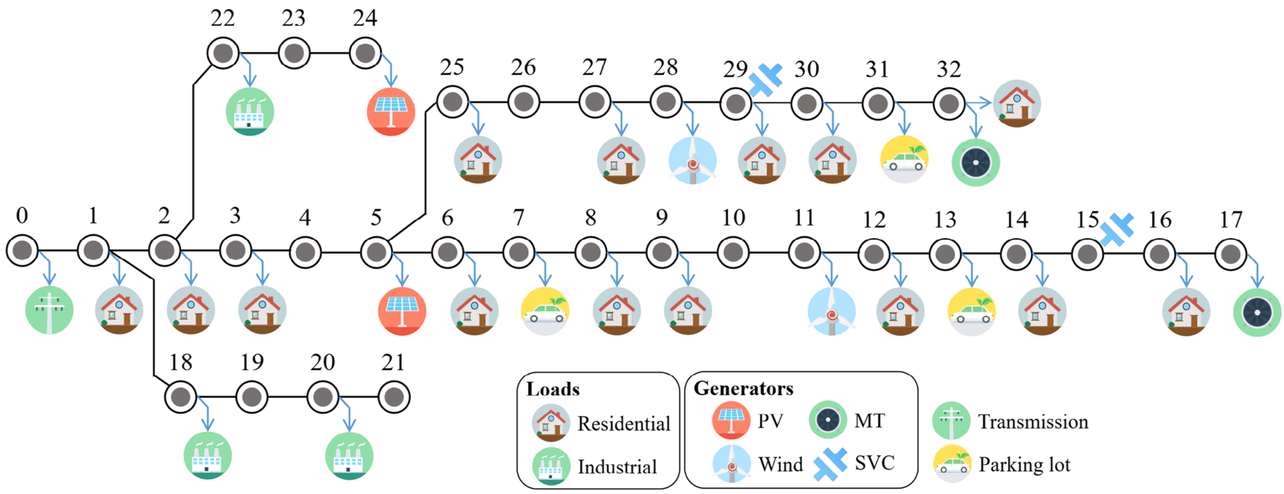

FIGURE 4 The modified 33-bus radial distribution system considered in simulations.

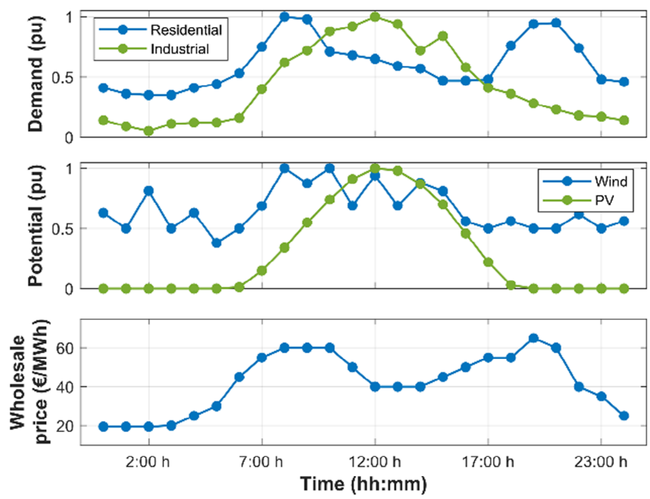

FIGURE 5 Per-unit demand (top), per-unit renewable potential (middle) and wholesale electricity price (bottom) considered in the 33-bus case.

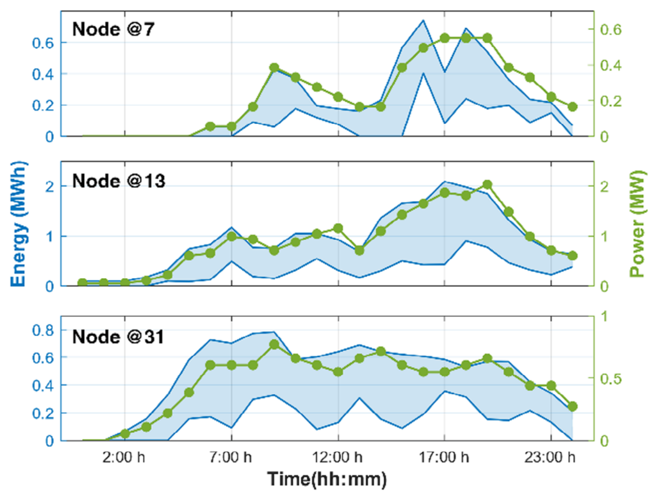

FIGURE 6 PL data considered in the 33-bus case.

TABLE 4 MT and SVC data.

	MTs		SVCs	
	@17	@32	@15	@29
Rated power	0.6 MVA	0.6 MVA	0.5 Mvar	0.5 Mvar
Fuel cost	40€/MWh	60€/MWh	–	–

TABLE 5 Some results obtained in the 33-bus case.

	NC (€)	Fuel cost (€)	Imports (MWh)	Charging (MWh)
Case 1	1908	413.5	33.15	7.07
Case 2	2019	0	43.14	7.07
Case 3	2690	434.9	50.42	7.07

while $a^{\mathrm{ex}} = 0.7$, typical of power systems with high renewable penetration [45]. MTs are installed at nodes 17 and 32, while SVCs are installed at nodes 15 and 29, similar to [28], whose data are reported in Table 4.

Three PLs are considered at nodes 7, 13 and 31. SOC bounds and power limits are plotted in Figure 6, and have been built following the methodology in [6] considering different parking sizes and 55-kW charging points, typical rated power for fast-chargers. We consider a battery efficiency of 95%, typical value of Li-ion technology [46], and a charging cost of 0.5€/kWh, typical of fast-charging stations [47].

5.2.1 | Overall results

Firstly, we present various economic and energy results in Table 5. Focusing on the network operation cost, not surprisingly, the lowest cost was obtained in Case 1, when DGs are enabled. It is clear that DGs provide an economic local

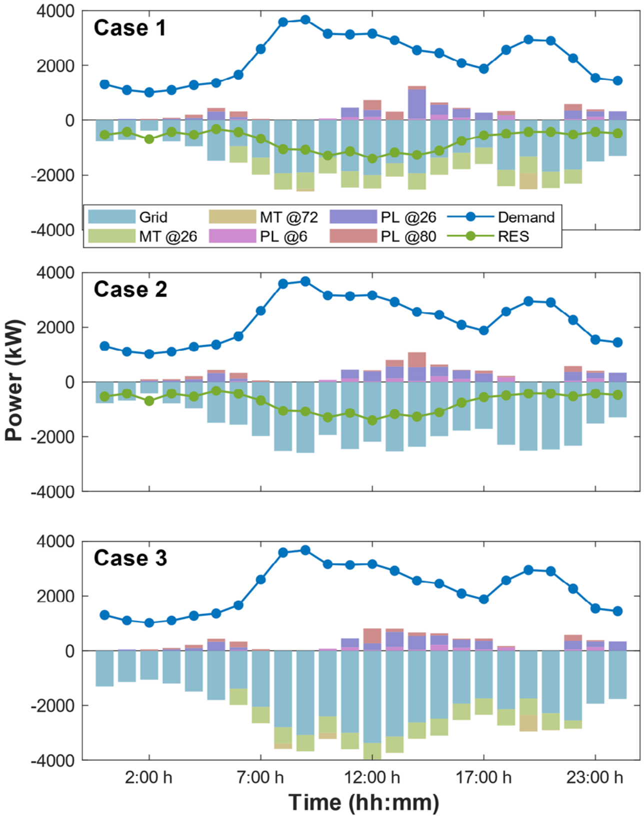

FIGURE 7 Scheduling results in the 33-bus case (negative power stands for generation).

generation option, which helps to reduce the total energy imported, as seen in the fourth column. Actually, energy imported in Case 1 reduces by 23 and 34% when compared with cases 2 and 3, respectively. As expected, the worst results were obtained in Case 3, when cheap generation through renewable generators was disabled. In the face of this situation, the distribution network makes use of MTs more frequently, increasing the total fuel cost.

More remarkably, the total energy charged by PLs was the same in the three cases studied. Therefore, it can be concluded that the developed model implicitly considers the strategic behaviour of PLs in the network operation. Indeed, considering PLs as strategic players gives to their profit maximization a high importance. This particular behaviour explains why PLs were able to charge the same energy even under very unfavourable conditions (e.g. in Case 3).

5.2.2 | Scheduling analysis

Next, we present the scheduling results for different assets in Figure 7. When renewable generators are enabled (cases 1 and 2), peak charging consumption is observed at 14:00 h, when high renewable potential coincides with a low demand period. As expected, this effect vanishes in Case 3, when charging demand is more displaced to midday, when low wholesale prices are observed. While it is clear that peak charging demand is

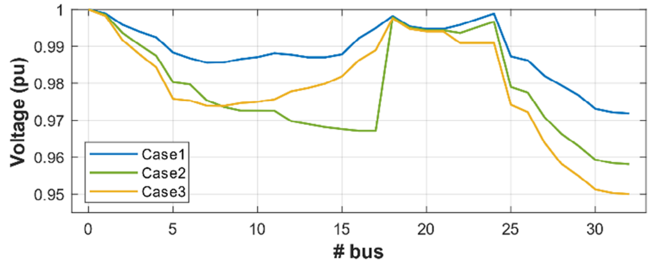

FIGURE 8 Per-unit voltages in the 33-bus case.

observed at afternoon, when more EVs are plugged at the same time, other charging periods are observed at night and evening in all the three cases studied. This is due to the same reasons previously exposed since at these hours low prices and demand periods coincide on time. Actually, PLs are directly supplied from the transmission system since renewable potential is low and MTs are not profitable due to the fuel cost is higher than wholesale electricity prices. Just for further validating the model, it is worth noting that MT at node 33 is much less operated than that at node 18. Actually, this MT is operated at evening barely, when wholesale electricity price is higher than its fuel cost.

5.2.3 | Voltage profile

Figure 8 plots nodal voltages in the three studied cases. Not surprisingly, full availability of distributed generation in Case 1 gives a better voltage profile compared to the other cases, enabling local generation and thus reducing voltage drop across branches. When compared the cases 2 and 3, it is worth noting that voltage drops further between nodes 10–16 in Case 2, while low voltages are observed across nodes 22–33 in Case 3. This is due to, in Case 2, MT at node 17 is disabled, thus lowing voltage support from this generator. In contrast, when renewable generators are disabled in Case 3, the branch 25–33 losses voltage support from the wind turbine installed at node 28.

5.3 | The 85-bus case

Next, we further validate the developed proposal in the 11-kV 85-bus case shown in Figure 9, whose branch data can be found in [48]. In this case, residential and industrial loads are not shown in Figure 9 for easing its visualization, but were distributed in the following way: according to [48], peak loads take 14, 35.28, 56, or 112 kW. In our particular case, we consider the same loads at the same nodes as in [48], considering that 14 and 35.28 kW loads are residential demand, while the rest are industrial consumers, considering the base profiles as in Figure 5. Due to peak demand in this system is much lower than in the 33-bus case, we consider the same number of DGs and SVCs with the same features. PLs and the rest of data are exactly the same as in the 33-bus case, while nominal powers for renewable generators are shown in Table 6.

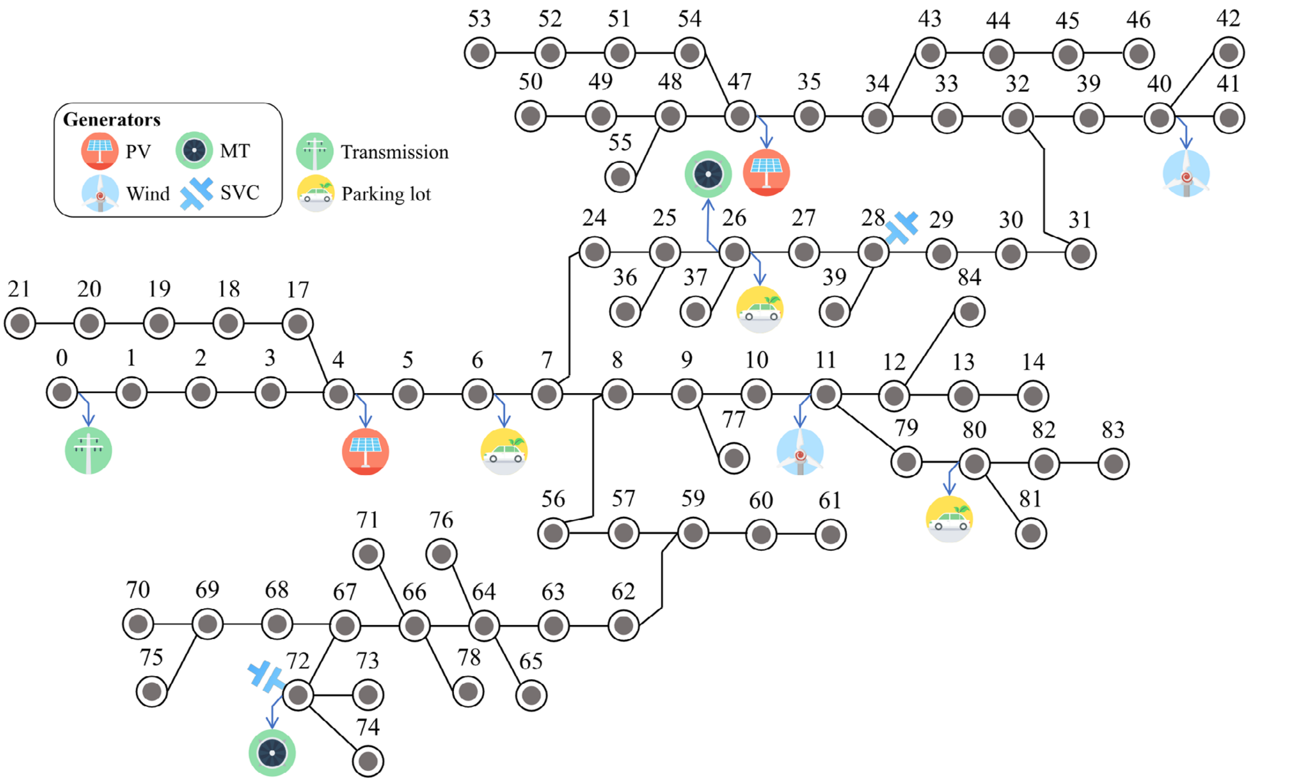

FIGURE 9 The 85-bus radial distribution system considered in simulations.

TABLE 6 Renewable generators nominal power in the 85-bus case.

Node	Nominal power (kW)
@4	300
@11	400
@40	450
@47	300

TABLE 7 Some results obtained in the 85-bus case.

	NC (€)	Fuel cost (€)	Imports (MWh)	Charging (MWh)
Case 1	837	439.5	9.6	7.07
Case 2	947	0	20.1	7.07
Case 3	1617	516.9	25.8	7.07

5.3.1 | Overall results

Table 7 is analogue to Table 5 but referred to the 85-bus case. As observed, the same can be concluded in this case but remarking the fact that PLs charged exactly the same energy in this case, further confirming that the developed model is capable to effectively consider the strategic behaviour of PLs in ADNs. Regarding the rest of results, it is interesting to see that total energy imported increases by 52 and 63% in cases 2 and 3, more notably than in the 33-bus case. This is due to disabling DGs has a higher impact in larger distribution systems due to voltage and flow constraints throughout the network, hindering the possibility of locally supplying some nodes that must necessarily import energy directly from the transmission system.

5.3.2 | Scheduling analysis

Next, we present the scheduling results for the 85-bus case in Figure 10. As seen, charging demand suppose a larger portion of total demand compared to the 33-bus case, due to residential and industrial demands are lower in this system. For the rest of the results, one can conclude the same as for the 33-bus case, just mentioning that the system is able to export electricity at 2:00 h in cases 1 and 2, due to peak wind potential and very low demand.

5.3.3 | Voltage profile

Lastly, Figure 11 plots the per-unit nodal voltage in the 85-bus case. As in the 33-bus system, the best voltage profile is observed in Case 1. In Case 3, a further voltage drop occurs through branches 28–54, due to renewable generators installed at nodes 40 and 47 are disabled. In contrast, lower voltages are observed between nodes 56–75 in Case 3, due to voltage support from the MT at node 72 is lost in this case.

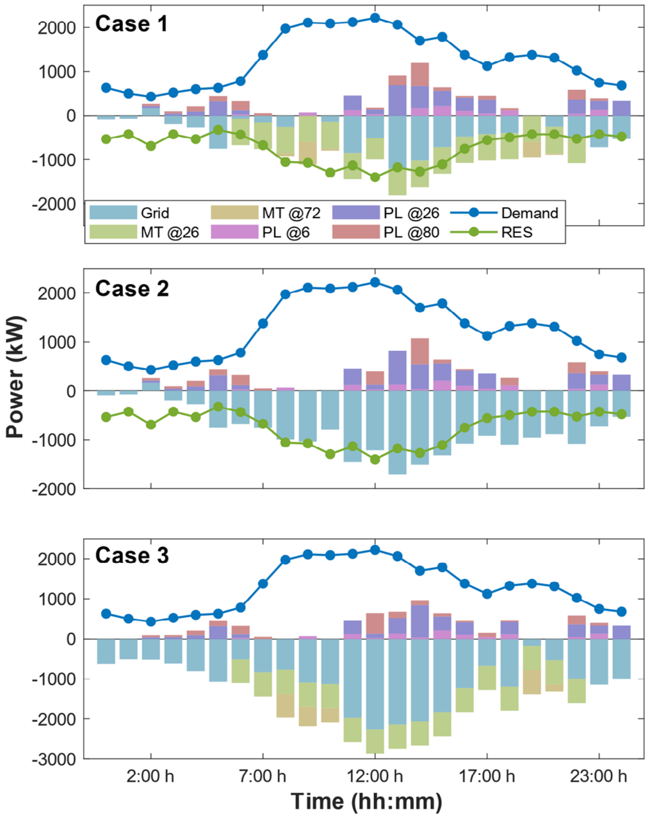

FIGURE 10 Scheduling results in the 85-bus case (negative power stands for generation).

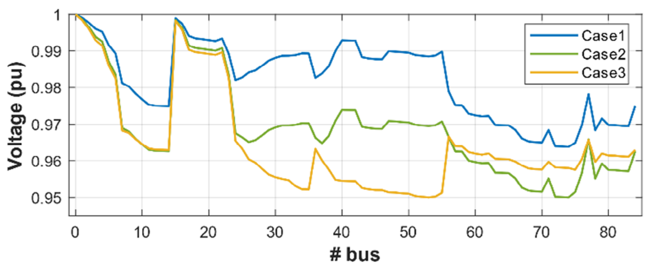

FIGURE 11 Per-unit voltages in the 85-bus case.

5.4 | Sensitivity analysis

Now, we provide a sensitivity analysis regarding residential, industrial loads and renewable generators. To this end, base demand and renewable potential are multiplied by real factors α^D and α^{RES}, respectively. The results for this analysis in the two considered systems are shown in Figures 12 and 13. As observed, the results reported further validate the developed model, giving coherent solutions in all the studied cases. Indeed, the network operation cost decreases with α^{RES} and increases with α^D in the two studied cases, following the same behaviour that the fuel cost and energy imported. This is due to high renewable potential enables large local generation capability, which allows reducing the energy imported from the transmission system and the output of MTs. On contrary, incrementing

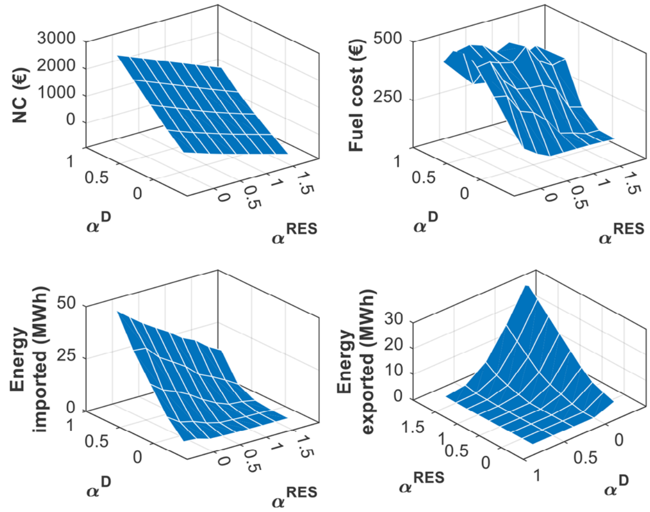

FIGURE 12 Sensitivity analysis in the 33-bus case.

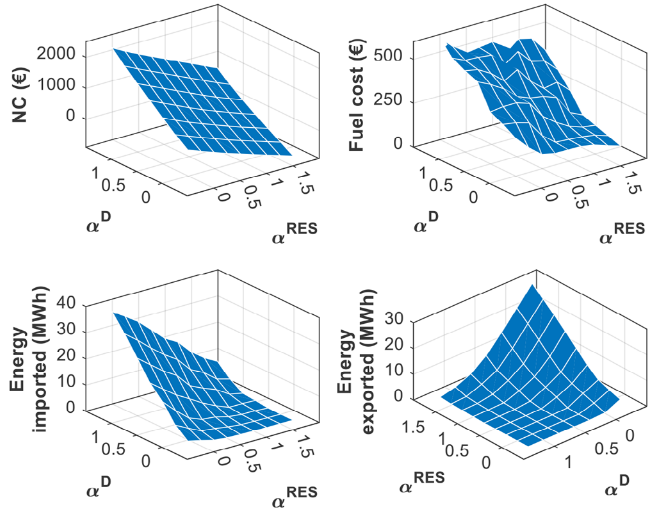

FIGURE 13 Sensitivity analysis in the 85-bus case.

the demand level gives rise the opposite trending, requiring to import more energy from the transmission system. On the other hand, unlike to the energy imported, exports increase with α^{RES} and decreases until zero with α^D.

5.5 | Computational performance

Finally, we assess the computational performance of the developed tool with the objective of validating it for industrial and real-life applications. To this end, various simulations were run on an Intel Core i7-10700K CPU 3.80 GHz 3.79 GHz with 32 GB RAM, reporting the average computational time in Table 8. As seen, computational time remains below 20 seconds in all the cases studied, which is more than reasonable for day-ahead tools that are performed with daily periodicity. Moreover, it is interesting to note that increment on time in the 85-bus system is not critical, thus demonstrating that the developed model scales well with the size of the system.

TABLE 8 Average computational time (in seconds) in all the cases studied.

	33-bus	85-bus
Case 1	11.1	18.0
Case 2	12.7	19.7
Case 3	12.1	19.7

5.6 | Comparison with metaheuristics

The developed mathematical model is a MILP and therefore can be solved using exact techniques like branch-and-bound methods. This kind of techniques are normally preferred as the global optimum reachability is ensured. This way, the use of other heuristic approaches is not justified at all. Nevertheless, we performed some preliminary experiments comparing the results obtained using exact methods, as in the results reported above, and the metaheuristic proposed in [49]. The numerical results were similar in both cases, however, the metaheuristic required much more time to converge to a valid solution. Moreover, this technique revealed to be few reliable, leading to different solutions between consecutive runs, frequently. Therefore, we recommend the use of exact techniques, requiring the use of heuristics only when the mathematical model results strongly nonlinear.

6 | CONCLUSIONS AND FUTURE WORKS

A novel energy management model for active distribution networks has been developed. The main novelty lies in integrating strategic behaviour of parking lots into network-level decisions, thus ensuring that the network scheduling plan does not detract monetary incentives of parking owners. To this end, an original tri-level game equilibrium framework has been developed. The original intractable multi-level structure has been reduced to a tractable single-level MILP by combining equivalent primal-dual and first-order optimality conditions of the distribution network and parking models.

The new proposal has been validated on well-known 33-, and 85-bus radial distribution systems under different demanding scenarios. Results demonstrate that the developed tool is capable of ensuring the parking profit even under unfavourable conditions with limited distributed generation. This result indicated that particular interests of parking owners are preserved implicitly, thus constituting a more profitable management strategy. Moreover, different studies have been conducted to demonstrate that the new proposal performs well under different demand and renewable penetration and scales well with the size of the system

Future research should be devoted on developing novel energy management tools that leverage further capabilities offered by electric vehicles. For instance, their energy arbitrage capability may provide further flexibility in network operation. Monetary incentives will be investigated in order to encourage the participation of parking lots in this kind of programs.

NOMENCLATURE

Sets (indices)

T (t)	Time
J (j, k)	Nodes
D (d)	Loads
$G^{\mathrm{MT/RES}}$ (g)	Microturbines/renewable generators
C (c)	Parking lots
S (s)	Static var compensators
$\Omega_j^{D/G/C/S}$	Set of loads/generators/parking lots/static var compensators connected to the jth node in the network
Ψ_j/Φ_j	Set of nodes downstream/upstream from the jth node in the network
N (n)	Breakpoints for linearization of second-order cone constraints
J_ω	Indicates the node to which the ωth is connected

Superscripts

im/ex	Imports/exports
P/Q	Active/reactive flows
$\underline{(\cdot)}/\overline{(\cdot)}$	Minimum/maximum value of a variable or parameter
$\widetilde{(\cdot)}$	Forecasted

Parameters

W	Wholesale electricity price (€/kWh)
a^{ex}	Reduction in selling price (pu)
L	Fuel cost (€/kWh)
V^0	Voltage at the root node (V)
R/X	Branch resistance/inductance (ohm)
$\bar{S}_g$	Rated power of the gth microturbine (kVA)
$\tilde{p}_{g,t}$	Potential of the gth renewable generator at time t (kW)
γ	Parameters for linearization of second-order cone constraints (-)
F	Charging price (€/kWh)
$C_{c,t}^0$	Energy stored in vehicles arriving to the cth parking lot at time t (kWh)
$\bar{C}_{c,t}^E$	Capacity of vehicles leaving the cth parking lot at time t (kWh)
M	Large positive constant (-)

Decision variables (primal)

p/q	Active/reactive power injection (kW/kvar)
SOC	Energy (kWh)
f	Power flow (kW/kvar)
V	Nodal voltage (V)

ψ Auxiliary variables to linearize complementarity conditions (binary)

Decision variables (dual)

$\lambda/\varphi/\phi$ Dual variables linked to equality constraints (€/kWh)

$(\underline{\zeta}/\bar{\zeta})/(\underline{\mu}/\bar{\mu})$ Dual variables linked to inequality constraints (€/kWh)

AUTHOR CONTRIBUTIONS

Marcos Tostado-Véliz: Conceptualization; data curation; formal analysis; funding acquisition; investigation; methodology; project administration; software; validation; writing—original draft; writing—review and editing. **Rohit Bhakar**: Conceptualization; formal analysis; methodology; resources; supervision; validation; visualization; writing—review and editing. **Mohammad Sadegh Javadi**: Data curation; supervision; visualization; writing—original draft. **Ali Esmaeel Nezhad**: Conceptualization; data curation; formal analysis; methodology; supervision; visualization. **Francisco Jurado**: Data curation; project administration; funding acquisition; formal analysis; supervision; visualization; writing—review & editing.

ACKNOWLEDGEMENTS

Marcos Tostado-Véliz and Francisco Jurado acknowledge to the Spanish Ministry of Science and Innovation, under the research Project "Development of power-flow models for microgrid clusters" PID2021-123633OB-C31, Ministry of Science and Innovation, Knowledge Generation Projects 2021, Spain. Marcos Tostado-Véliz acknowledges to University of Jaén for funding his international research stay at the Institute for Systems and Computer Engineering, Technology and Science (INESC TEC) under his program 'Ayudas para estancias breves del personal investigador en formación para la obtención del doctorado con mención internacional (Acción 6)'. Moreover, he wishes to thank to Institute for Systems and Computer Engineering, Technology and Science (INESC TEC) for hosting this stay, during which this work was conceptualized. Mohammad Sadegh Javadi acknowledges Fundação para a Ciência e a Tecnologia (FCT) for his contract funding provided through 2021.01052.CEECIND.

CONFLICT OF INTEREST STATEMENT

The authors declare no conflicts of interest.

DATA AVAILABILITY STATEMENT

Data sharing is not applicable to this article as no datasets were generated or analysed during the current study.

ORCID

Rohit Bhakar https://orcid.org/0000-0003-0155-9327
Ali Esmaeel Nezhad https://orcid.org/0000-0002-6522-4043
Francisco Jurado https://orcid.org/0000-0001-8122-7415

REFERENCES

1. European Commission. 2050 long-term strategy. https://climate.ec.europa.eu/eu-action/climate-strategies-targets/2050-long-term-strategy_en. Accessed 8 May 2024
2. International Energy Agency. CO2 emissions by sector. https://www.iea.org/regions/europe/emissions. Accessed 8 May 2024
3. Nasir, M., Jordehi, A.R., Matin, S.A.A., Tabar, V.S., Tostado-Véliz, M., Mansouri, S.A.: Optimal operation of energy hubs including parking lots for hydrogen vehicles and responsive demands. J. Energy Storage. 50, 104630 (2022). https://doi.org/10.1016/j.est.2022.104630
4. New Mercedes station offers 400-kW fast-charging, more than EVs can even handle car and driver. https://www.caranddriver.com/news/a45847770/mercedes-chargepoint-fast-ev-charging-stations/ (2023). Accessed 8 May 2024
5. Tostado-Véliz, M., Jordehi, A.R., Zhou, Y., Mansouri, S.A., Jurado, F.: Best-case-aware planning of photovoltaic-battery systems for multi-mode charging stations. Renewable Energy 225, 120300 (2024). https://doi.org/10.1016/j.renene.2024.120300
6. Tostado-Véliz, M., Jordehi, A.R., Mansouri, S.A., Jurado, F.: A two-stage IGDT-stochastic model for optimal scheduling of energy communities with intelligent parking lots. Energy 263(D), 126018 (2023). https://doi.org/10.1016/j.energy.2022.126018
7. Amini, F., Ghassemzadeh, S., Rostami, N., Tabar, V.S.: A stochastic two-stage microgrid formation strategy for enhancing distribution network resilience against earthquake event incorporating distributed energy resources, parking lots and responsive loads. Sustainable Cities Soc. 101, 105191 (2024). https://doi.org/10.1016/j.scs.2024.105191
8. Zheng, Y., Yu, H., Shao, Z., Jian, L.: Day-ahead bidding strategy for electric vehicle aggregator enabling multiple agent modes in uncertain electricity markets. Appl. Energy 280, 115977 (2020). https://doi.org/10.1016/j.apenergy.2020.115977
9. Mirzaei, M.J., Kazemi, A., Homaee, O.: A probabilistic approach to determine optimal capacity and location of electric vehicles parking lots in distribution networks. IEEE Trans. Ind. Inf. 12(5), 1963–1972 (2016). https://doi.org/10.1109/TII.2015.2482919
10. Sattarpour, T., Farsadi, M.: Parking lot allocation with maximum economic benefit in a distribution network. Int. Trans. Elect. Energy Syst. 27(1), e2234 (2017). https://doi.org/10.1002/etep.2234
11. Amini, M.H., Moghaddam, M.P., Karabasoglu, O.: Simultaneous allocation of electric vehicles' parking lots and distributed renewable resources in smart power distribution networks. Sustainable Cities Soc. 28, 332–342 (2017). https://doi.org/10.1016/j.scs.2016.10.006
12. Fathy, A., Abdelaziz, A.Y.: Competition over resource optimization algorithm for optimal allocating and sizing parking lots in radial distribution network. J. Cleaner Prod. 264, 121397 (2020). https://doi.org/10.1016/j.jclepro.2020.121397
13. Mozaffari, M., Askarian Abyaneh, H., Jooshaki, M., Moeini-Aghtaie, M.: Joint expansion planning studies of EV parking lots placement and distribution network. IEEE Trans. Ind. Inf. 16(10), 6455–6465 (2020). https://doi.org/10.1109/TII.2020.2964049
14. Yang, J., Xiong, J., Chen, Y.-L., Yee, P.L., Ku, C.S., Babanezhad, M.: Improved golden jackal optimization for optimal allocation and scheduling of wind turbine and electric vehicles parking lots in electrical distribution network using Rosenbrock's direct rotation strategy. Mathematics 11(6), 1415 (2023). https://doi.org/10.3390/math11061415
15. Turan, M.T., Ates, Y., Erdinc, O., Gokalp, E., Catalão, J.P.S.: Effect of electric vehicle parking lots equipped with roof mounted photovoltaic panels on the distribution network. Int. J. Elect. Power Energy Syst. 109, 283–289 (2019). https://doi.org/10.1016/j.ijepes.2019.02.014
16. Haghifam, S., Najafi-Ghalelou, A., Zare, K., Shafie-khah, M., Arefi, A.: Stochastic bi-level coordination of active distribution network and renewable-based microgrid considering eco-friendly compressed air energy storage system and intelligent parking lot. J. Cleaner Prod. 278, 122808 (2021). https://doi.org/10.1016/j.jclepro.2020.122808
17. Karimi-Arpanahi, S., Jooshaki, M., Pourmousavi, S.A., Lehtonen, M.: Leveraging the flexibility of electric vehicle parking lots in distribution

networks with high renewable penetration. Int. J. Elect. Power Energy Syst. 142(B), 108366 (2022). https://doi.org/10.1016/j.ijepes.2022.108366
18. Haji-Aghajani, E., Hasanzadeh, S., Heydarian-Forushani, E.: A novel framework for planning of EV parking lots in distribution networks with high PV penetration. Electr. Power Syst. Res. 217, 109156 (2023). https://doi.org/10.1016/j.epsr.2023.109156
19. Nasiri, N., Zeynali, S., Ravadanegh, S.N., Kubler, S.: Moment-based distributionally robust peer-to-peer transactive energy trading framework between networked microgrids, smart parking lots and electricity distribution network. IEEE Trans. Smart Grid 15(2), 1965–1977 (2024). https://doi.org/10.1109/TSG.2023.3296917
20. Baherifard, M.A., Kazemzadeh, R., Yazdankhah, A.S., Marzband, M.: Intelligent charging planning for electric vehicle commercial parking lots and its impact on distribution network's imbalance indices. Sustainable Energy Grids Networks 30, 100620 (2022). https://doi.org/10.1016/j.segan.2022.100620
21. Alizadeh, M., Jafari-Nokandi, M., Shahabi, M.: Resiliency improvement of distribution network considering the charge/discharge management of electric vehicles in parking lots through a bilevel optimization approach. Int. Trans. Elect. Energy Syst. 2022, 1–20 (2022). https://doi.org/10.1155/2022/3878440
22. Khodadadi, A., Abedinzadeh, T., Alipour, H., Pouladi, J.: Optimal resilient operation of smart distribution network in the presence of renewable energy resources and intelligent parking lots under uncertainties. Int. J. Elect. Power Energy Syst. 147, 108814 (2023). https://doi.org/10.1016/j.ijepes.2022.108814
23. Alizadeh, M., Jafari-Nokandi, M.: A bi-level resilience-oriented islanding framework for an active distribution network incorporating electric vehicles parking lots. Electr. Power Syst. Res. 218, 109233 (2023). https://doi.org/10.1016/j.epsr.2023.109233
24. Amini, F., Gassemzadeh, S., Rostami, N., Tabar, V.S.: A stochastic two-stage microgrid formation strategy for enhancing distribution network resilience against earthquake event incorporating distributed energy resources, parking lots and responsive loads. Sustainable Cities Soc. 101, 105191 (2024). https://doi.org/10.1016/j.scs.2024.105191
25. Ruiz, C., Conejo, A.J., Smeers, Y.: Equilibria in an oligopolistic electricity pool with stepwise offer curves. IEEE Trans. Power Syst. 27(2), 752–761 (2012). https://doi.org/10.1109/TPWRS.2011.2170439
26. Naebi, A., Shenava, S.J.S., Contreras, J., Ruiz, C., Akbarimajd, A.: EPEC approach for finding optimal day-ahead bidding strategy equilibria of multi-microgrids in active distribution networks. Int. J. Elect. Power Energy Syst. 117, 105702 (2020). https://doi.org/10.1016/j.ijepes.2019.105702
27. Qiao, D., Wang, G., Xu, M.: Fast-charging station location problem: a two-phase approach with mathematical program with equilibrium constraints considering charging choice behavior. Sustainable Cities Soc. 96, 104678 (2023). https://doi.org/10.1016/j.scs.2023.104678
28. Wang, X., Li, F., Zhang, Q., Shi, Q., Wang, J.: Profit-oriented BESS siting and sizing in deregulated distribution systems. IEEE Trans. Smart Grid 14(2), 1528–1540 (2023). https://doi.org/10.1109/TSG.2022.3150768
29. Tostado-Véliz, M., Liang, Y., Jordehi, A.R., Mansouri, S.A., Jurado, F.: An interval-based bi-level day-ahead scheduling strategy for active distribution networks in the presence of energy communities. Sustainable Energy Grids Networks 35, 101088 (2023). https://doi.org/10.1016/j.segan.2023.101088
30. Noutash, A., Kalantar, M.: Resilience enhancement with transportable storage systems and repair crews in coupled transportation and distribution networks. Sustainable Cities Soc. 99, 104922 (2023). https://doi.org/10.1016/j.scs.2023.104922
31. Javadi, M.S., Lotfi, M., Nezhad, A.E., Anvari-Moghaddam, A., Guerrero, J.M., Catalão, J.P.S.: Optimal operation of energy hubs considering uncertainties and different time resolutions. IEEE Trans. Ind. Appl. 56(5), 5543–5552 (2020). https://doi.org/10.1109/TIA.2020.3000707
32. Gurobi Optimization L.L.C. Gurobi optimizer reference Manual. https://www.gurobi.com (2021). Accessed 9 May 2024
33. Akbari, T., Bina, M.T.: Linear approximated formulation of AC optimal power flow using binary discretization. IET Gener., Transm. Distrib. 10(5), 1117–1123 (2016). https://doi.org/10.1049/iet-gtd.2015.0388
34. Dvorkin, V., Fioretto, F., Van Hentenryck, P., Pinson, P., Kazempour, J.: Differentially private optimal power flow for distribution grids. IEEE Trans. Power Syst. 36(3), 2186–2196 (2021). https://doi.org/10.1109/TPWRS.2020.3031314
35. Tostado-Véliz, M., Hasanien, H.M., Jordehi, A.R., Turky, R.A., Jurado, F.: Risk-averse optimal participation of a DR-intensive microgrid in competitive clusters considering response fatigue. Appl. Energy 339, 120960 (2023). https://doi.org/10.1016/j.apenergy.2023.120960
36. Mitridati, L., Kazempour, J., Pinson, P.: Heat and electricity market coordination: a scalable complementarity approach. Eur. J. Oper. Res. 283(3), 1107–1123 (2020). https://doi.org/10.1016/j.ejor.2019.11.072
37. Tostado-Véliz, M., Hasanien, H.M., Jordehi, A.R., Turky, R.A., Gómez-González, M., Jurado, F.: An Interval-based privacy – aware optimization framework for electricity price setting in isolated microgrid clusters. Appl. Energy 340, 121041 (2023). https://doi.org/10.1016/j.apenergy.2023.121041
38. Wu, X., Conejo, A.J.: Distribution market including prosumers: an equilibrium analysis. IEEE Trans. Smart Grid 14(2), 1495–1504 (2023). https://doi.org/10.1109/TSG.2022.3151338
39. Fortuny-Amat, J., McCarl, B.: A representation and economic interpretation of a two-level programming problem. J. Oper. Res. Soc. 32(9), 783–792 (1981). https://doi.org/10.1057/jors.1981.156
40. Kleinert, T., Schmidt, M.: Global optimization of multilevel electricity market models including network design and graph partitioning. Discrete Optim. 33, 43–69 (2019). https://doi.org/10.1016/j.disopt.2019.02.002
41. Pinson, P., Han, L., Kazempour, J.: Regression markets and application to energy forecasting. TOP. 30, 533–573 (2022). https://doi.org/10.1007/s11750-022-00631-7
42. 33-bus test system. https://www.torontomu.ca/content/dam/cue/research/reports/33bus%20test%20system.pdf. Accessed 8 May 2024
43. Tostado-Véliz, M., et al.: Risk-averse electrolyser sizing in industrial parks: an efficient stochastic-robust approach. Appl. Energy 367, 123389 (2024). https://doi.org/10.1016/j.apenergy.2024.123389
44. Tostado-Véliz, M., Jordehi, A.R., Mansouri, S.A., Jurado, F.: Day-ahead scheduling of 100% isolated communities under uncertainties through a novel stochastic-robust model. Appl. Energy 328, 120257 (2022). https://doi.org/10.1016/j.apenergy.2022.120257
45. Engie. Historical data reports. https://www.engieresources.com/historical-data#reports_anchor. Accessed 8 May 2024
46. Hasanien, H.M., Alsaleh, I., Tostado-Véliz, M., Alassaf, A., Alateeq, A., Jurado, F.: Optimal parameters estimation of lithium-ion battery in smart grid applications based on gazelle optimization algorithm. Energy 285, 129509 (2023). https://doi.org/10.1016/j.energy.2023.129509
47. Tostado-Véliz, M., Kamel, S., Hasanien, H.M., Arévalo, P., Turky, R.A., Jurado, F.: A stochastic-interval model for optimal scheduling of PV-assisted multi-mode charging stations. Energy 253, 124219 (2022). https://doi.org/10.1016/j.energy.2022.124219
48. Das, D., Kothari, D.P., Kalam, A.: Simple and efficient method for load flow solution of radial distribution networks. Int. J. Elect. Power Energy Syst. 17(5), 335–346 (1995). https://doi.org/10.1016/0142-0615(95)00050-0
49. Nemati, M., Braun, M., Tenbohlen, S.: Optimization of unit commitment and economic dispatch in microgrids based on genetic algorithm and mixed integer linear programming. Appl. Energy 210, 944–963 (2018). https://doi.org/10.1016/j.apenergy.2017.07.007

How to cite this article: Tostado-Véliz, M., Bhakar, R., Javadi, M.S., Esmaeel Nezhad, A.E., Jurado, F.: Integrating the strategic response of parking lots in active distribution networks: an equilibrium approach. IET Renew. Power Gener. 19, e13195 (2025). https://doi.org/10.1049/rpg2.13195